

Role of conventional proton magnetic resonance spectroscopy in the outcome prediction of neonatal hypoxic-ischemic encephalopathy

Doctoral dissertation

Hajnalka Bognárné Barta MD

Semmelweis University
Rácz Károly Doctoral School of Clinical Medicine



Supervisor: Miklós Szabó MD, Ph.D, med. habil.

Official reviewers: Kinga Karlinger MD, Ph.D, D.Sc
Gyula Tálosi MD, Ph.D

Head of the Complex Exam Committee: László Rosivall MD, Ph.D, D.Sc

Members of the Complex Exam Committee: Barna Vásárhelyi MD, Ph.D, D.Sc
András Fogarasi MD, Ph.D, D.Sc
László Szabó MD, Ph.D, med. habil.

Budapest
2021

Table of contents

Table of contents	2
List of abbreviations	5
1 Introduction	7
1.1 Hypoxic-ischemic encephalopathy	7
1.1.1 Epidemiology and etiology.....	7
1.1.2 Pathophysiology	8
1.1.3 Clinical presentation	11
1.1.4 Neuroprotection	14
1.2 Role of imaging techniques in the diagnosis and prognosis of HIE.....	17
1.2.1 Cranial ultrasound	17
1.2.2 Magnetic resonance	17
1.3 Proton MR spectroscopy.....	20
1.3.1 Metabolites	20
1.3.2 Cerebral metabolism registered by H-MRS	22
1.3.3 Prognostic value of H-MRS	23
1.4 Outcomes following HIE	25
1.4.1 Assessment of neurological sequelae	25
1.4.2 Cerebral palsy	26
2 Objectives	30
2.1 Predictive value of early, conventional brain H-MRS in neonatal HIE	30
2.2 Optimal postnatal age at H-MRS for outcome prediction in newborns with HIE	30
2.3 Dynamic changes of brain H-MRS metabolite ratios in neonatal HIE.....	30
2.4 Prevalence and clinical manifestation of CP at Semmelweis University	31

3	Methods	32
3.1	Patient selection	32
3.1.1	Predictive value of early, conventional H-MRS in neonatal HIE	32
3.1.2	Optimal postnatal age at H-MRS for outcome prediction in HIE	34
3.1.3	Dynamic changes of H-MRS metabolite ratios in neonatal HIE	34
3.1.4	Prevalence and clinical presentation of CP at Semmelweis University ...	36
3.2	Clinical care of newborns with HIE.....	37
3.3	Brain H-MRS examination	37
3.3.1	Metabolites and metabolite ratios.....	38
3.3.2	H-MRS analysis.....	38
3.3.3	Predictive value of early, conventional brain H-MRS in neonatal HIE ...	39
3.3.4	Optimal postnatal age at H-MRS for outcome prediction in HIE	40
3.3.5	Dynamic changes of H-MRS metabolite ratios in neonatal HIE.....	40
3.4	Neurodevelopmental outcome	40
3.5	Statistical analysis	41
3.5.1	Predictive value of early, conventional brain H-MRS in neonatal HIE ...	41
3.5.2	Optimal postnatal age at H-MRS for outcome prediction in neonatal HIE 42	
3.5.3	Dynamic changes of H-MRS metabolite ratios in neonatal HIE.....	42
3.5.4	Prevalence and clinical presentation of CP at Semmelweis University ...	42
3.6	Ethical considerations	42
4	Results	44
4.1	Predictive value of early, conventional brain H-MRS in neonatal HIE	44
4.2	Optimal postnatal age at H-MRS for outcome prediction in neonatal HIE.....	52
4.3	Dynamic changes of H-MRS metabolite ratios in neonatal HIE.....	56
4.4	Prevalence and clinical presentation of CP at Semmelweis University	58

5	Discussion.....	62
5.1	Optimization of outcome prediction with conventional H-MRS in newborns with HIE	62
5.1.1	Limitations.....	66
5.2	Prevalence and clinical presentation of CP at Semmelweis University	67
5.2.1	Limitations.....	69
6	Conclusion.....	71
7	Summary.....	72
8	Összefoglalás.....	73
9	Bibliography	74
10	Bibliography of the candidate’s publications	84
10.1	Publications related to the thesis:	84
10.2	Publications not related to the thesis:	84
11	Acknowledgements	85

List of abbreviations

ADC: apparent diffusion coefficient
ADP: adenosine-diphosphate
aEEG: amplitude-integrated electroencephalogram
AR/IVF: assisted reproduction/*in vitro* fertilisation
ATP: adenosine-triphosphate
AUC: area-under-the-ROC-curve
BD: base deficit
BGT: basal ganglia/thalamus
BS: burst suppression
CFCS: Communication Function Classification System
Cho: choline
CI: confidence interval
CNV: continuous normal voltage
CP: cerebral palsy
Cr: creatine
Cr2: secondary creatine peak
DNV: discontinuous normal voltage
DTI: diffusion tensor imaging
DWI: diffusion-weighted imaging
EDACS: Eating and Drinking Ability Classification System
Epo: erythropoietin
FT: flat trace
Glx: glutamate/glutamine
GMFCS: Gross Motor Function Classification System
HIE: hypoxic-ischemic encephalopathy
H-MRS: proton magnetic resonance spectroscopy
HT: hypothermia treatment
ICD: International Classification of Diseases
IUGR: intrauterine growth restriction
IQR: interquartile range

Lac: lactate
Lip: lipid
LV: low voltage
MACS: Manual Ability Classification System
MDI: mental developmental index
mI: myo-inositol
MR: magnetic resonance
MRI: magnetic resonance imaging
MRS: magnetic resonance spectroscopy
n: sample size
NAA: N-acetyl-aspartate
NICU: neonatal intensive care unit
NOS: nitric oxide synthase
PA: perinatal asphyxia
PCr: phosphocreatine
PDI: psychomotor developmental index
PLIC: posterior limb of internal capsule
P-MRS: phosphorous magnetic resonance spectroscopy
post-PA CP: cerebral palsy after perinatal asphyxia/hypoxic-ischemic encephalopathy
ppm: parts per million
PRESS: Point RE-Solved Spectroscopy
ROC: Receiver-Operating Curve
SCPE: Surveillance of Cerebral Palsy in Europe collaboration
SD: standard deviation
SGA: birthweight small for gestational age
SNR: signal-to-noise ratio
SUPC: sudden unexpected postnatal collapse
TE: echo time
TOBY: Total Body Hypothermia for Neonatal Encephalopathy clinical trial
TR: repetition time
VOI: volume of interest
 X^2 : chi-square statistic

1 Introduction

1.1 Hypoxic-ischemic encephalopathy

1.1.1 Epidemiology and etiology

Perinatal asphyxia (PA) and consequential hypoxic ischemic encephalopathy (HIE) is a severe and mostly unpredictably occurring condition of the perinatal period, with a prevalence ranging from 1.5‰ in developed countries to as high as 26‰ in the developing world (1). Moreover, HIE is responsible for the death of yearly 0.7 million newborns worldwide, and several million children develop consequential permanent neurological deficit each year (2). Neonates affected with milder forms of HIE are often underdiagnosed, yet still recover completely, without any permanent neurological damage in the majority. However, 10-15% of newborns with moderate-to-severe HIE die from the complications of the condition, 10-15% of surviving children develop cerebral palsy (CP), and further 40-50% show different psychomotor and mental developmental deficits (e.g. hearing or visual loss, autism spectrum disorders, epilepsy, mental retardation etc.) (3).

The timing of the hypoxic-ischemic insult is categorized based on the time period of occurrence – this affects the success of neuroprotection, and also plays a role in the resulting neuropathology and presented symptoms –: (a) prepartum/intrauterine, (b) intrapartum and (c) postpartum events (4). The principal *intrapartum events* leading to HIE include acute placental and umbilical disturbances (e.g. placental abruption or cord prolapse), prolonged labor with transverse arrest (e.g. due to abnormal presentation or shoulder dystocia), difficult instrumental extraction or rotational maneuvers (e.g. breech maneuver), and other acute intrapartum events compromising maternal cardiovascular stability (e.g. maternal hemorrhage, rupture of uterus or general anesthesia) (5). *Postpartum events* alone can also lead to HIE, caused by various neonatal respiratory and cardiovascular conditions (e.g. severe recurrent apneic cells, circulatory insufficiency secondary to patent ductus arteriosus or other congenital heart diseases), manifesting in the form of sudden unexpected postnatal collapse (SUPC), an entity that occurs in 0.3-0.8/1000 livebirths (6). Postpartum asphyxia is one of the possible etiologies in the

background of SUPC, and might contribute to all cases of HIE by approximately 10% (7). However, these factors are much more important in the pathogenesis of encephalopathy in preterm infants. *Prepartum/intrauterine events* leading to HIE are mainly related to abnormal placental/cord function, caused by various conditions (e.g. placental vasculopathy, delayed villous chorionic maturation, chronic chorioamnionitis or funisitis secondary to maternal infection, intrauterine growth retardation, maternal diabetes, preeclampsia) (8). Evidence quantifying the relative contribution of these factors to the total prevalence of HIE is rather controversial. While a magnetic resonance imaging (MRI) study estimated the prevalence of antenatally acquired insults around 5%, others hypothesize that antenatal factors are present in 96% of HIE cases, with or without a concomitant intrapartum acute hypoxic insult (9,10). The explanation for these contradictory findings is that although some acute prepartum events can indeed directly lead to HIE (e.g. maternal hypotension or hemorrhage, severe placental abnormality), most of these previously listed prenatal factors sensitize and predispose for a subsequent intrapartum injury, by compromising placental flow. That being said, these data need to be interpreted with the awareness that determination of the timing of the insult is usually based on imprecise methods (4).

1.1.2 Pathophysiology

The fundamental cause of neural tissue disturbance in HIE is the deficit of substrate supply, i.e. oxygen. The perinatal brain can be deprived of oxygen by two means: *hypoxia* and consequential *hypoxemia*, constituting a diminished blood oxygen level, as well as *ischemia*, which is diminished blood supply to the brain. Experimental as well as clinical data suggest that ischemia has the more important role of these two pathophysiological factors, considering that deprivation of oxygen as well as glucose and other substrates are crucial in the pathogenesis of the condition (4). The biochemical and metabolic processes following the hypoxic-ischemic insult can be divided in three stages:

Primary energy failure occurs immediately during the hypoxic-ischemic insult, as a direct consequence. Depletion of oxygen inhibits the mitochondrial oxidative phosphorylation, resulting in decreasing level of adenosine-triphosphate (ATP) in neurons. Automatically, anaerobic glycolysis is activated in order to maintain energy production, however, at a much lower level (while oxidative phosphorylation produces 38 molecules of ATP from

a single molecule of glucose, anaerobic glycolysis can only produce 2). Consequently, accumulation of lactate and protons occurs, causing tissue acidosis. Initially, this constitutes an adaptive response to the hypoxic-ischemic insult, since decreasing pH induces the hydrolysis of phosphocreatine (PCr), the main form of high-energy phosphate in the brain. Exhaustion of ATP increases levels of adenosine-monophosphate (AMP), which in turn accelerates anaerobic glycolysis, as well as glycogenolysis in astrocytes, in order to provide sufficient glucose substrate from glycogen for the increased needs of glycolysis. These adaptive changes are capable of temporarily maintaining neuronal metabolism, for 1-2 hours following the hypoxic-ischemic insult (see *Figure 1*) (11,12).

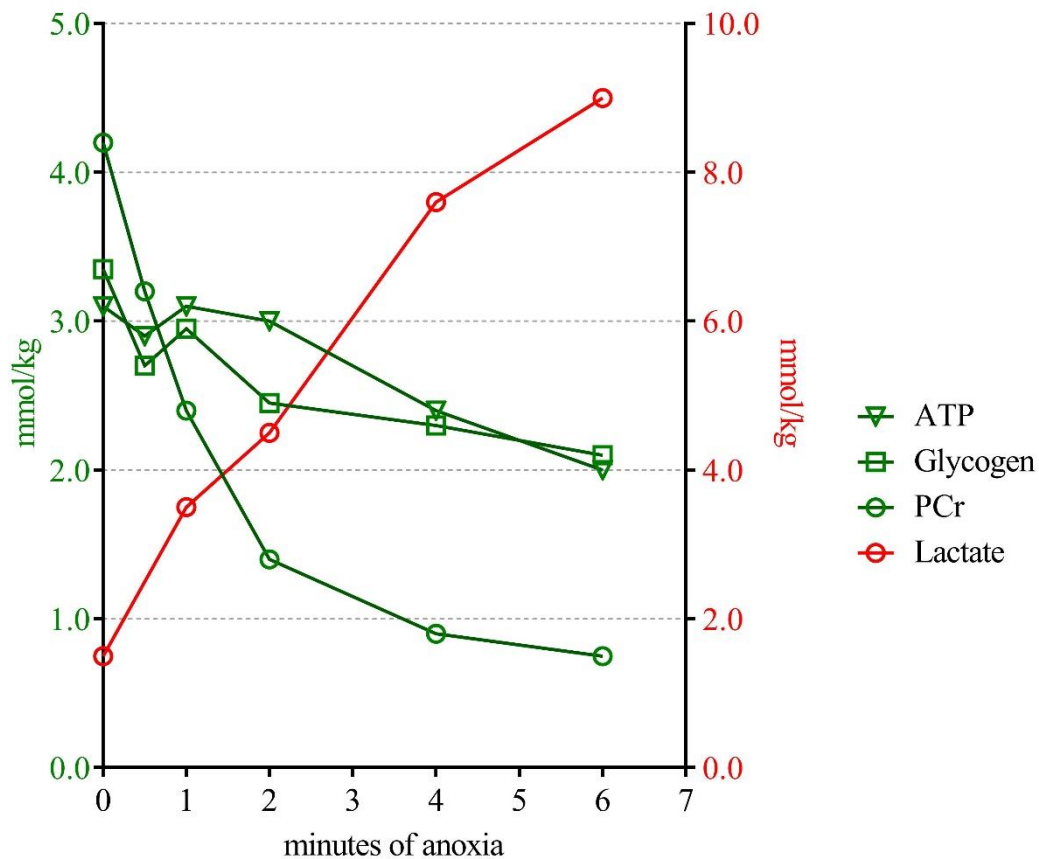


Figure 1. Biochemical effects of hypoxemia, following the primary energy failure. Concentrations of metabolites in the brain of newborn mice, by duration of anoxia (adapted from data published by *Holowach-Thurston et al* (11)). Left Y-axis (green font): concentration of adenosine-triphosphate (ATP), glycogen, phosphocreatine (PCr); right Y-axis (red font): concentration of lactate.

However, with progression of lactate formation and increasing acidosis, several deleterious effects occur, namely (a) impairment of cerebral autoregulation, a potential

for further ischemic injury, (b) inhibition of phosphofructokinase, which provides the pyruvate substrate for anaerobic glycolysis, as well as (c) direct cellular injury and necrosis due to tissue acidosis. Meanwhile, the initial decrease of neural ATP causes the failure of ATP-dependent $\text{Na}^+\text{-K}^+$ pump, which is crucial for the homeostasis of cells. Consequent intracellular Na^+ , Ca^{2+} and water accumulation occurs, resulting in cytotoxic edema and membrane depolarization, causing excessive release of glutamate, which in turn results in further intracellular Ca^{2+} accumulation, generating free radicals and activating phospholipase, which begins the degradation of cellular lipids (13,14). Mitochondrial permeability is also increased, which releases several apoptosis-inducing factors into the cell (15). On top of that, reoxygenation and consequential oxidative stress enhance the deleterious events described previously (4). All these pathways enhance each other and ultimately lead to neuronal apoptosis and necrosis. All these impairments of cell metabolism manifest clinically called as *delayed or secondary energy failure*, occurring 6-8 hours after the hypoxic-ischemic insult, with its nadir around 24-48 hours, and lasting for several days, based on in vivo human brain phosphorous MR spectroscopy observations (16). The cell level events contributing to the secondary energy failure are presented in *Figure 2*.

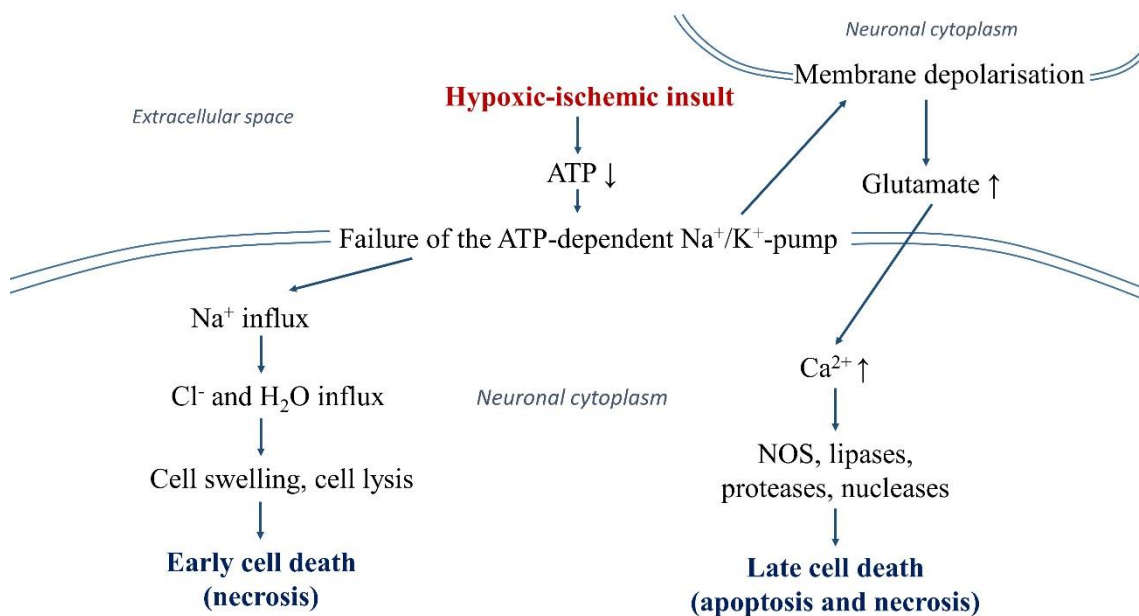


Figure 2. Pathogenesis of the secondary energy failure, following the hypoxic-ischemic insult. Adapted from data published by Kusaka *et al*, Barks *et al* and Gilland *et al* (13-15). ATP: adenosine-triphosphate, NOS: nitric oxide synthase.

Latest evidence suggests that in case of severe neuronal damage and insufficient recovery, activation of inflammatory response persists, and abnormal proliferation of glial cells (gliosis) as well as various epigenetic changes occur (17). These mechanisms contribute to lasting cerebral lactic acidosis, which fuel the above detailed pathological processes. This persisting neurological deterioration is the *tertiary phase* of the hypoxic-ischemic pathophysiology, lasting from weeks to years (18).

1.1.3 Clinical presentation

The neurological signs and symptoms of the hypoxic-ischemic insult of the brain usually appear right after birth. These symptoms are not specific for HIE, but rather show the state of functional impairment of the brain, and may appear in other forms of neonatal encephalopathies, as well (4). The succession of neurological signs following the hypoxic insult has been described in detail by *Sarnat & Sarnat*, detailing the systemic reactions triggered by hypoxia/ischemia (19). Characteristics of the three Sarnat stages are presented in *Table 1*.

After the onset of the acute hypoxic-ischemic insult, adrenal activation occurs, rising plasma catecholamine levels, in order to counteract the imminent circulatory insufficiency. This explains the hyperalertness characterizing *Stage 1* of HIE, which might be the only neurological syndrome seen in newborns having suffered only mild hypoxic injury. However, in case of moderate-to-severe HIE, this stage is brief and usually undergoes *in utero* (marked by fetal tachycardia). The subsequent *Stage 2* is mainly characterized by parasympathetic overactivity, likely caused by the release from inhibition of the brainstem, spinal cord reflexes, vagal and other parasympathetic nerve functions. This stage is characterized by lower level of consciousness, represented by lower electric brain activity on electroencephalogram (EEG), and often by appearance of seizures. In cases where *Stage 2* undergoes *in utero*, it is represented by the fetal bradycardia following the tachycardia. *Stage 3* is the extension of this parasympathetic overactivity throughout the neuraxis, manifesting in absent muscle tone and reflexes, stuporous consciousness, temporary lack of seizures and lengthening isoelectric phases on EEG. While newborns with mild HIE might not undergo Stages 2-3 at all, babies with moderate-to-severe HIE might present with symptoms of Stages 2-3 right after delivery (19).

Table 1. Sarnat staging of newborns with hypoxic-ischemic encephalopathy (19).
EEG: electroencephalogram.

	Sarnat stage 1	Sarnat stage 2	Sarnat stage 3
Duration of stage	Less than 24 h	2 to 14 days	Hours to weeks
Level of consciousness	Hyperalert	Lethargic or obtunded	Stuporous
<i>Neuromuscular control</i>			
Muscle tone	Normal	Mild hypotonia	Flaccid
Posture	Mild distal flexion	Strong distal flexion	Intermittent decerebration
Stretch reflexes	Overactive	Overactive	Decreased or absent
Segmental myoclonus	Present	Present	Absent
<i>Complex reflexes</i>			
Suck	Weak	Weak or absent	Absent
Moro	Strong; low threshold	Weak; incomplete; high threshold	Absent
Oculovestibular	Normal	Overactive	Weak or absent
Tonic neck	Slight	Strong	Absent
Autonomic function	Generalized sympathetic	Generalized parasympathetic	Both systems depressed
Pupils	Mydriasis	Miosis	Variable; often unequal; poor light reflex
Heart rate	Tachycardia	Bradycardia	Variable
Bronchial and salivary secretions	Sparse	Profuse	Variable
Gastrointestinal motility	Normal or decreased	Increased; diarrhea	Variable
Seizures	None	Common: focal or multifocal	Uncommon (excluding decerebration)
EEG findings	Normal (awake)	Early: low-voltage continuous delta and theta. Later: periodic pattern (awake). Seizures: focal 1-to 1½-Hz spike-and-wave	Early: periodic pattern with isopotential phases. Later: totally isopotential

Besides the above described original Sarnat staging, several simpler neurological scoring systems were developed, like the modified Sarnat EEG score (20) or the Thompson score (21). However, the main limitation of these scoring systems is the difficulty of assessing certain neurological signs (e.g. primitive reflexes) right after birth, and the problematic interpretation of some intermediate signs, that often do not fit in any of the categories. Moreover, the neurological signs visible to the clinician are strongly affected by medication and may be altered by other biochemical abnormalities (e.g. acidosis, glucose

level), emphasizing that while these scoring systems are fundamental in the immediate clinical diagnosis of HIE, they are fairly imprecise and therefore not suitable for prediction of long-term outcome (22).

Therefore, the previously mentioned EEG and more importantly, **amplitude-integrated EEG (aEEG)** is a highly valuable tool to refine the assessment of the severity of encephalopathy, as well as signs of early recovery. The latter has the important advantage of being a user-friendly and point-of-care method easily attained by the neonatal intensive care personnel (23). The aEEG trace is classified based on voltage and pattern in the following main categories: continuous normal voltage (CNV), discontinuous normal voltage (DNV), burst suppression (BS), continuous low voltage (LV) and flat trace (FT) (24).

Although previously, we focused on the pathological processes and clinical symptoms of the central nervous system, the effects of the perinatal hypoxic-ischemic insult impair several organ systems, causing various organ dysfunctions, or even multi-organ failure. These disturbances can be manifested in acute tubular necrosis, hepatopathy, myocardial impairment and cardiovascular insufficiency, pulmonary hypertension, gastrointestinal dysfunction or coagulopathy, indicated by non-specific laboratory parameters, like rising creatinine, blood urea nitrogen, transaminases or creatine kinase, as well as hyperkalemia, hypocalcemia, laboratory signs of coagulopathy and frequently, rising markers of inflammation, without an infectious background (25). While abnormalities of the central nervous system are detected in 20% of symptomatic cases of PA, and 60% present both neurological and other organ dysfunctions, in 20% of cases, only extracerebral organ injury appears without any neurological signs (26).

Generally, the diagnosis of moderate-to-severe HIE is established combining the information gained from the peripartum history and degree of acidosis, a thorough clinical examination of neurological signs and symptoms, as well as the result of aEEG monitoring. The gold standard diagnostic criteria has been outlined by the international Total Body Hypothermia for Neonatal Encephalopathy (TOBY) clinical trial (27), which also constitute the criteria for hypothermia treatment (see *Table 2*).

Table 2. Diagnostic criteria for moderate-to-severe HIE, as well as eligibility criteria for hypothermia treatment.

The presence of A and B criteria is sufficient to establish the diagnosis of moderate-to-severe HIE, and commence cooling. The C criterion is used to aid the diagnosis; however, since availability of aEEG is limited in certain centers, it is not routinely applied everywhere. BD: base deficit, aEEG: amplitude-integrated electroencephalography.

A criteria	<ul style="list-style-type: none"> • Apgar score ≤ 5 at 10 min after birth OR • continued need for resuscitation (including endotracheal or mask ventilation) at 10 min after birth OR • acidosis (pH < 7.0) OR BD ≥ 16 mmol/L within 60 min after birth (occurring in any umbilical, arterial or capillary blood sample)
B criteria	<ul style="list-style-type: none"> • altered level of consciousness (lethargy, stupor or coma) AND at least one of the following: <ul style="list-style-type: none"> • hypotonia OR • abnormal reflexes (including oculomotor and pupil reflexes) OR • absent or weak suck OR • clinical seizures
C criterion	<ul style="list-style-type: none"> • abnormal brain background activity or seizures registered on at least 30 minutes of aEEG recording

1.1.4 Neuroprotection

1.1.4.1 Hypothermia treatment

The efficacy and safety of hypothermia treatment (HT) has been closely studied since the 1990s, resulting in HT being the current gold standard neuroprotective method for newborns with moderate-to-severe HIE (28). Based on the results of the multicenter TOBY trial, moderate whole-body hypothermia of 33-34 °C maintained for 72 hours decreased the combined risk of death or adverse neurological sequelae by 19% (27). This decrease in mortality and morbidity presumes that HT was introduced in the first 6 postnatal hours of eligible infants, as cooling induced after 6 hours of life is hypothesized to be ineffective (29). The eligibility criteria for HT is identical to the diagnostic criteria of moderate-to-severe HIE used in the majority of neonatal intensive care units (NICUs), described in detail in *Table 2*.

The therapeutic process is divided into three phases: (a) *induction*, where the target temperature is rapidly achieved, together with close monitoring of blood pressure, plasma glucose and blood gas levels; (b) *maintenance phase*, where core temperature needs to be

kept as stable as possible, with maximal fluctuation of ± 0.5 °C; and (c) *rewarming phase*, where the temperature increase velocity must be kept below 0.2-0.5 °C/h, to prevent hypoglycemia, hypokalemia and acidosis (30). To inhibit shivering, and alleviate the discomfort caused by cooling, infants undergoing HT usually need major analgesia and sedation (31).

The working mechanism of HT lies in slowing enzymatic cellular processes (based on the Van't Hoff's law), therefore reducing cerebral metabolism (and thus glucose and oxygen utilization) by 5% per °C (32). This decreases the consequential accumulation of anaerobic metabolites, excitatory amino-acids and reactive free radicals, which would potentially lead to neuronal injury and death (33).

Despite its promising utility in preventing the development of long-term neurological deficits or death, the number needed to treat in case of HT is 8, and approximately half of the infants receiving whole-body cooling still have an abnormal outcome, suggesting that a significant portion of newborns with the most severe injuries may not be rescued (34). This underscores the need for further, additional or alternative neuroprotective methods besides HT.

1.1.4.2 New emerging neuroprotective methods

Several recent preclinical and clinical studies has drawn attention to other emerging neuroprotective strategies, briefly discussed below.

Melatonin is an endogenous neuroendocrine molecule regulating the circadian rhythm, and also influencing a number of developmental and immunological processes (18). Its neuroprotective effect is presumably achieved via anti-apoptotic, anti-inflammatory and anti-oxidative processes, promoting neuronal and glial development. A recent randomized control study with 80 enrolled HIE infants concluded that a single dose of 10 mg melatonin reduced mortality by more than 60% (35). As for neurological sequelae, another study revealed that HIE newborns receiving both melatonin and HT presented fewer seizures on EEG and had less white matter injury on MRI, than infants treated with HT alone, corroborated the boosting effect between multiple neuroprotective strategies (36).

Erythropoietin (Epo) has – besides its well-known effect of inducing red blood cell production – a vital role in promoting proliferation and differentiation of neuronal, glial and endothelial cells throughout the central nervous system. Moreover, it has been described that Epo receptors are upregulated following brain injury, supporting Epo’s role in endogenous neuroprotection (37). Evidence shows that Epo might help stimulate reparatory mechanisms in the tertiary phase of HIE, with its optimal administration window between the first days and weeks of life. Randomized controlled trials suggest that Epo treatment alone reduces the risk of CP by about 50%, compared to HT alone, and MRI performed in HIE newborns treated with a combination of Epo and HT show lower volumes of brain injury, than infants receiving HT alone (38).

Remote ischemic postconditioning exploits the organism’s endogenous protective mechanisms, and is described by intermittent sublethal interruptions to blood flow, in a non-vital organ (e.g. a limb), remote to the affected organ (i.e. the brain) (39). This controlled limb ischemia triggers the release of a number of endogenous autacoids (e.g. kinins), affects the immune response (e.g. reduces neutrophil activation), and decreases expression of apoptotic and inflammatory genes. This results in increasing cerebral flow, attenuation of neuroinflammation and activation of pro-survival signaling cascades at cell-level (40). Animal studies suggest that four 10-minute cycles of lower limb ischemia/reperfusion protected effectively against white matter injury, when started immediately after resuscitation (41). However, clinical safety and reproducibility studies are still needed, in order to determine the recommended and safe dose of controlled remote ischemia, with or without HT.

A number of additional neuroprotective agents are currently studied, including cannabinoids, xenon, topiramate or allopurinol, and further candidates are constantly emerging (42). However, as mentioned before, the temporal factor in introducing neuroprotective methods is crucial in all potentially effective interventions, emphasized by the commonly used phrase “time is brain” (43). This underscores the ultimate need not only for the early diagnosis of HIE, but also for the precise determination of severity as well as the accurate prediction of outcome, as soon as possible. Therefore, risk stratification in HIE is of utmost importance, in order to select HIE newborns who would benefit the most from future compound neuroprotective strategies (44).

1.2 Role of imaging techniques in the diagnosis and prognosis of HIE

The diagnosis of moderate-to-severe encephalopathy is usually corroborated by imaging techniques, especially useful in ruling out other etiologies additional to HIE, that could modulate the clinical appearance, or interfere with therapy (4).

1.2.1 Cranial ultrasound

Cranial ultrasound is routinely used in neonatology, due to its safety and availability at the bedside, however, it has poor interobserver reproducibility and its sensitivity greatly depends on the examiner (45). While the guidelines of the American Academy of Neurology consider cranial ultrasound as the first line imaging technique principally for the diagnosis of intracranial hemorrhage and intracranial congenital malformations, it has also some value in HIE, especially for differential diagnostic purposes, i.e. quick exclusion of other etiologies for encephalopathy (46). Additionally, Doppler cerebral flow velocity and resistance indices are commonly used to estimate cerebral flow. Its disturbances are sensitive markers of the severe hypoxic brain injury and may add a lot to the information provided by cranial ultrasound alone (47).

1.2.2 Magnetic resonance

Magnetic resonance (MR) and its various modalities are considered the gold standard radiological technique to diagnose neonatal HIE. MRI, its imaging modality, provides detailed anatomic and neuropathological pictures of the brain, due to its excellent tissue differentiation, moreover, its functional modalities (functional MRI and MR spectroscopy) offer unique information on the metabolic and functional state of the brain, in a non-invasive way (48).

The biophysical foundation of MR lies in the magnetic characteristics of protons, which are organized and aligned when placed in a strong magnetic field (i.e. the MR scanner). During the MR scan, excitation of these aligned protons is achieved using radiofrequency wave, followed by relaxation and consequential release of the energetic surplus. The parameters of the relaxation are characteristic of the environment of the affected proton

(i.e. the tissue), which is scanned and reconstructed to create the MR images of the examined organ (49).

Current guidelines recommend the performance of at least 2 MR scans in newborns with HIE – ideally, an initial scan between postnatal hours 24-96, and a repeated, control scan after postnatal day 6 – considering that the utility and sensitivity of the different MR modalities vary with postnatal age (44). The main modalities, their strengths and weaknesses are briefly described in the following chapter.

1.2.2.1 MR modalities

MRI has been used for imaging in newborns with HIE for more than 30 years, accurately differentiating between the various morphological types of HIE, and also capable of estimating the timing of the hypoxic-ischemic insult. To improve comparability of scans, scoring systems were developed to grade the severity of HIE-related MRI abnormalities (50). Detection of injury to the basal ganglia and thalamus (BGT), as well as the signal change in the posterior limb of internal capsule (PLIC) are important predictors of adverse outcome in newborns with HIE (51). However, sensitivity of conventional MRI is greatly dependent of the timing of the scan, and MRI scans often appear normal during the very early days of life. As macroscopic lesions take time to develop, only injuries acquired prior birth are detectable with high confidence in this time frame (52). During the first week, pathophysiological maturation of perinatal injuries occur, as they become visible on MRI scans in the second half of the first week of life, confirming the full extent and pattern of the hypoxic ischemic insult (48).

Diffusion-weighted imaging (DWI) optimized the low sensitivity of MRI during the first days of life, enabling the detection of cytotoxic edema and consequential cell swelling, appearing days before morphological abnormalities are shown on conventional MRI (53). The accuracy of DWI is further improved by quantification of diffusion, using apparent diffusion coefficient (ADC), showing low ADC values for a more severe injury. Therefore, DWI examinations can provide early information for the diagnosis of HIE as well as for prediction of neurological outcome, when conventional MRI might still appear normal (54). However, as histopathological changes progress after the first week (i.e. vasogenic edema and loss of cell membrane integrity appear), the previously low ADC

values begin to rise, and temporarily reach the normal range, presenting the issue of pseudo-normalization. This process worsens the sensitivity of DWI and ADC in this time period (55).

Diffusion tensor imaging (DTI) and **tractography** are further developments of ways to detect diffusion, constructing a 3-dimensional diffusivity map to help identify the asymmetry of white matter, impaired microstructural organization of corpus callosum or the corticospinal tracts, and can thus predict poor long-term cognitive and motor performance (56).

MR angiography and venography are capable of visualizing the cerebral vascular system noninvasively, without the use of contrast material. These methods have contributed to the increased detection of sinovenous thrombosis in newborns (57).

Magnetic resonance spectroscopy (MRS) has been used for a long time, even before MRI emerged as an imaging technique. Its analytical utility to assess the chemical composition of a volume of interest (VOI) is based on the fact that atomic nuclei behave differently, have different magnetic parameters, and resonate differently, based on the chemical compound they are in, due to molecular interactions. Conclusively, the chemical composition of certain VOI is represented by a spectrum of curves, where the horizontal position of the spectral curve is specific to the chemical substance (or in case of brain MRS, the cerebral metabolite), shown in ppm (parts per million) units. Based on the acquired spectrum, metabolite concentration is proportional to the height of the spectral curve (peak height), as well as the area under the spectral curve (peak area) (58).

During the MRS acquisition, the time intervals of excitation-registration can be optionally modified by applying different echo times (TE). The level of noise, as well as the number of detectable metabolites can thus be fine-tuned, depending on the clinician's need. Lower TE settings enable the registration of only a few metabolites, with relatively low noise level. At higher TE settings though, more metabolite curves emerge from the spectrum, however, noise level also increases (59).

Chemical elements with atomic nuclei suitable for use in MRS are proton (H^+), phosphorous (^{31}P), fluorine (^{19}F), carbon (^{13}C) and sodium (^{23}Na). From these methods, only proton and phosphorous MRS are used in the routine clinical practice (60).

1.3 Proton MR spectroscopy

Proton MR spectroscopy (H-MRS) is a non-invasive tool to assess tissue functionality and metabolism in various conditions. In pediatric radiology, it is widely used in patients with HIE, epilepsy and metabolic diseases, but it also provides valuable information concerning the metabolic spectrum (and thus, malignant potential) of neoplasms and infectious processes involving various organs (e.g. liver), and above all, excel at the diagnostic workup of cerebral pathologies, such as white matter disorders (61).

The VOI of the examination can be freely determined, requiring a minimal volume of $1 \times 1 \times 1 \text{ cm}^3$, based on a conventional MR image. In HIE, the most common VOIs include the thalamus and basal ganglia, the cortex (although artifacts resulting from overlapping white matter or bone matter are difficult to prevent), as well as white matter (60).

1.3.1 Metabolites

As detailed earlier, the metabolic spectrum of the examined tissue can be acquired using various TE settings. Generally, brain H-MRS is registered at TE 35 ms, 144 ms and 288 ms. On the spectrum registered with brain H-MRS – as seen in *Figure 3.* –, the following main metabolite peaks can be distinguished:

N-acetyl-aspartate (NAA) is the second most abundant cerebral amino-acid (after glutamate), and can be found almost exclusively in neurons, with its peak registered at 2.01-2.02 ppm (62). Its role in the central nervous system is rather complex and still not fully understood; however, evidence suggests that this molecule functions as an osmolite, regulating the expulsion of intracellular fluid produced by normal metabolism, and thus prevents cell swelling (63). Moreover, it presumably plays a role in protein and lipid synthesis, by providing the source, storage and transport of acetyl-group, aspartate and amino-nitrogen (64). NAA levels increase rapidly with neuronal maturation during gestation, and especially during the first year of life, reaching its nadir around 3-5 years of life (65). Decreasing NAA level is a reliable marker of neuronal injury or dysfunction, even in the absence of cell death (66).

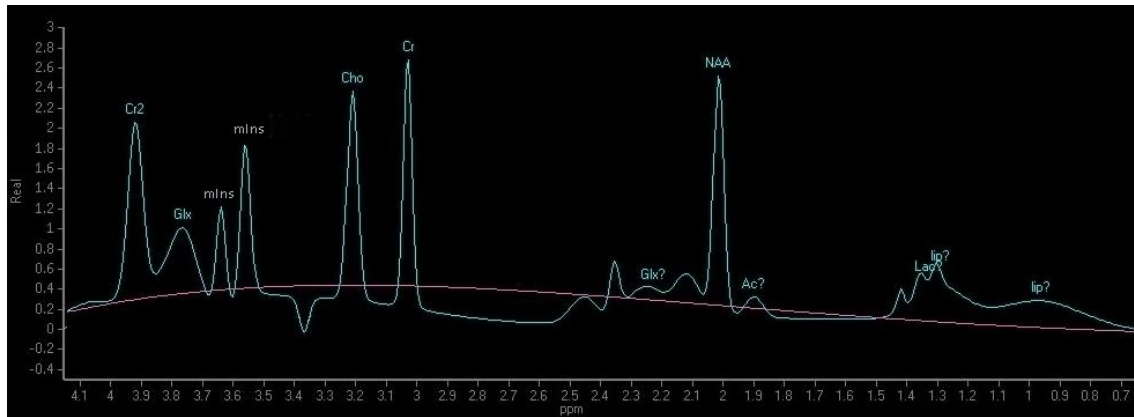


Figure 3. Spectrum acquired by H-MRS.

The registered metabolites are from left to right: Cr2: secondary creatine peak, Glx: glutamine/glutamate (multiple peaks, here: double peaks), mIns: myo-inositol (double peaks), Cho: choline, Cr: creatine, NAA: N-acetyl-aspartate, Lac: lactate.

? represent low (< 1) signal-to-noise ratio (SNR).

Creatine (Cr) is a non-neuron-specific substance, synthesized primarily in the liver and kidneys, which is then phosphorylated into PCr, and transported into organs with high energetic needs, such as muscles and the brain. The utility of PCr lies in re-converting adenosine-diphosphate (ADP) produced during ATP utilization into ATP, thus significantly increasing usability of the available cellular energy pool. Due to its function, Cr is an important marker of the examined tissue's energy status (67). Cr and PCr levels increase rapidly before and around term, and contrary to other metabolites, their levels stay relatively constant after the first year of life (65). Due to its special energetic characteristics, two Cr peaks appear on the spectrum (Cr and Cr2). Because of its better differentiation from noise and other peaks, the first Cr peak is routinely used (measured around 3.0-3.1 ppm).

Choline (Cho) is a normal component of myelin sheath and neuronal cell membrane; therefore, its level in newborns is high – due to ongoing myelination –, and slowly decreases with age and with completion of myelination, reaching its final value at 3-5 years of age (65). The above normal Cho-concentration in the perinatal period might suggest degradation of central nervous system cells (both neuronal and glial) (61). The peak of Cho can be registered at 3.2 ppm.

Myo-inositol (mI or mIns) is a configuration variant of the pentose sugar inositol, not specific for the central nervous system. It functions as a precursor for inositol-derived lipid synthesis and is part of the intracellular second-messenger system (68). To date,

studies suggest that mI could be the breakdown product of abnormal cerebral inositol-polyphosphate metabolism and the cell membrane component myelin (69), implementing that increased mI levels signal cell death. In the neonatal period, mI is one of the highest peak, and rapidly decreases with age, reaching its final value around 1 year of age (65). The peak of mI can only be detected at TE = 35 ms and 144 ms, as a peak triplet (summation of three, partly overlapping peaks, registered between 3.45-3.65 ppm).

Glx (glutamine/glutamate) is the most abundantly found metabolite detectable with H-MRS in the brain, being an important neurotransmitter. Its level does not change significantly with age; however, due to the multiple Glx peaks resonating within the spectrum (multiplet peak), as well as their overlapping with other metabolite peaks does not allow Glx to be accurately and reliably measurable for diagnostic purposes (65).

Lac (lactate) is barely detectable in the central nervous system under normal conditions. Its importance lies in case of anaerobic metabolism, therefore, rise in its concentration is a classic sign of hypoxia and ischemia – both in neuronal and in other tissues (61). However, accurate detection of Lac peak is hindered by multiple issues. First, its peak cannot be detected at TE 35 ms due to high noise level, and TE 144 ms is only suitable for its assessment in severe cases of HIE, which result in extremely high lactate levels. Second, Lac peak is detected at 1.3 ppm, where it is superimposed on the broad lipid (Lip) peak, interfering with its measurement. Finally, introduction of HT as the gold standard neuroprotective method in HIE further inhibits precise use of Lac peak (70). This observation presumably indicates the working mechanism of HT, as it decelerates metabolic processes, and most importantly, glycolysis, delaying accumulation of lactate (71).

1.3.2 Cerebral metabolism registered by H-MRS

The non-invasiveness of H-MRS makes it a useful tool in monitoring metabolic changes undergoing in the brain of infants, after the hypoxic-ischemic insult. While repeated acquisition of H-MRS in same newborns has ethical limitations, the fluctuation of metabolites can be partly reconstructed based on the existing study results.

The events closely following the hypoxic-ischemic insult – i.e. during the primary energy failure – are difficult to observe, since it usually occurs *in utero* or during delivery.

However, on H-MRS spectra acquired in the first postnatal days, a prominent Lac peak, elevated Cho peak, as well as significantly decreased NAA and slightly reduced Cr peak can be seen in the thalamus of newborns with moderate-to-severe HIE, compared to the H-MRS spectra of healthy term newborns (72,73). As pathological processes progress during the first week, NAA levels keep sinking; however, repeated H-MRS up to postnatal weeks 4-5 show signs of recovery, signaled by higher NAA and Cr, as well as lower Cho peak, compared to the first postnatal days (74,75). Nevertheless, Lac peak has been described to persist for weeks after the insult, especially in newborns facing poor outcome, while Lac/NAA ratios slowly rise in the tertiary phase of the disease (i.e. after the first week, up to years), presumably due to the increasing NAA level (18).

1.3.3 Prognostic value of H-MRS

Previously, the prognostic value of H-MRS to predict 2-year-old neurodevelopmental outcome has been investigated by several studies in neonates with HIE, using various methods, protocols and equipment (54,76–85). Nevertheless, drawing a global conclusion applicable in the general clinical practice poses a problem, due to the difference of the methods and findings. Indeed, a wide range of H-MRS derived metabolites were suggested as potential biomarkers, e.g. some studies concluded that absolute Lac levels and/or Lac-containing metabolite ratios (Lac/NAA, Lac/Cho, Lac/Cr) were the most accurate for prediction of outcome (54,77–79,81–86), while others showed that NAA/Cr, NAA/Cho, absolute NAA and/or Cho levels had promising prognostic value (76,77,80,82,83), whereas only few studies investigated glutamate (Glx) or glutamate-containing metabolite ratios (Glx/Cr) (81), and/or mI (82).

Generalizability of these results is hindered by the variability of methods used, considering that some studies applied various data-optimizing software (80,83,87), methods for absolute metabolite quantification (79,80,85), or special head-coils (79,82) in order to improve the information acquired from the registered H-MRS spectra. While these methods may indeed ameliorate data quality, they are not generally applicable in standard clinical settings as there is no uniform consent on their use (88). Therefore, the diagnostic and prognostic workup of HIE using conventionally performed brain H-MRS needs to be specifically assessed, analyzing spectra acquired using a routine sequence on the average MR scanner.

As mentioned previously, both peak height and peak area are proportional with the metabolite concentration, and thus theoretically, can be used for comparison of metabolite levels. Despite their limitations, the majority of existing studies support the use of peak areas as prognostic markers in patients with HIE (86). Based on Bottomley's comprehensive review of H-MRS (89) though, without post-processing techniques, analysis of both peak height and peak area has certain challenges. While peak height provides an acceptable measure for non-overlapping metabolite peaks, it is affected by patient motion and inhomogeneous widening of spectrum widths. On the contrary, peak areas are relatively immune to motion artefacts and spectrum widening. Nevertheless, since most of the integrated area of a peak resides near its base, noise and overlapping of other peaks can significantly affect area measurements. Taking these aspects into consideration, under conventional circumstances, both peak heights and peak areas might have equal potential for outcome prediction.

1.4 Outcomes following HIE

Besides its life-threatening complications in the neonatal period, the significance of moderate-to-severe HIE lies in the imminent adverse neurological sequelae, ranging from mild delays in development to severe impairments, such as CP or mental retardation (4). Even with HT, almost half of surviving infants develop cognitive impairment (intelligence quotient < 70) or learning disabilities, and 17% are later diagnosed with CP (90). The incidence of visual disturbances (secondary amblyopia or blindness) is reported in 26% of cases, while hearing loss or deafness in 9% (91). Epilepsy develops in 10% of cases, usually by 3.5 years of age (92).

1.4.1 Assessment of neurological sequelae

Different aspects of outcome can be assessed at different ages. Severe motor or sensory loss is detectable as early as the first year of life, severe developmental delay in the second year, while fine and gross motor dysfunction between two to four years (depending on severity). However, some cognitive impairments become apparent only at later ages, since abnormalities in cognitive function can be assessed around four to seven years of age, while learning disabilities even later, between seven to nine years (93,94).

In our neonatal intensive care unit (NICU), all newborns diagnosed with moderate-to-severe HIE undergo referral to a neurodevelopment neurologist before discharge, and are routinely followed up around 2 years of age, using the Bayley Scales of Infant Development II tool-kit (95), performed by trained personnel (neurodevelopmental neurologist or pediatric psychologist). Parents or legal guardians of the children are routinely contacted via telephone for an appointment; participation on the follow-up examination is voluntary. This test evaluates psychomotor and mental development using various playful tasks and procedures, providing as a result the psychomotor (PDI) and mental developmental indices (MDI), which score development as follows: normal (≥ 85 points), mildly delayed (70-84 points), moderately delayed (55-69 points) or severely delayed (< 55 points) development. If needed, children are directed to specialized departments or developmental interventions.

1.4.2 Cerebral palsy

CP describes a group of permanent disorders of the development of movement and posture, causing activity limitation, which are attributed to non-progressive disturbances that occurred in the developing fetal or infant brain. The motor disorders of CP are often accompanied by disturbances of sensation, perception, cognition, communication and behavior, by epilepsy and by secondary musculoskeletal problems (96). Overall frequency of CP has been reported to be 1.5–2.7‰ by various countries (97); however, the national incidence in Hungary is unknown, only regional data are available, stating CP prevalence in Borsod-Abaúj-Zemplén county to be 2.1‰ (98).

Several pre-, intra- and postpartum events can potentially lead to CP, principally encompassing three causal pathways: (a) brain damage, (b) brain malformation and (c) functional disorders of the brain without any structural abnormality (97). The specific conditions are barely risk factors of CP, involving one or more pathways. Previously, intrapartum asphyxial insults were thought to be the main cause of CP; however, this hypothesis seems to be contradicted by recent epidemiological researches, revealing perinatal asphyxia in the background of only 20% of cases (99). Conversely, based on a systematic review of 27 studies in HIE, CP was diagnosed in 29% of HIE cases (91). Other risk factors of CP – besides HIE – include prematurity, intracranial hemorrhage, neonatal stroke, intrauterine growth restriction (IUGR), fetal inflammatory syndrome and infections of the central nervous system, cranial trauma, multiple pregnancy and assisted reproductive methods (97,100).

1.4.2.1 Clinical classification

Several classification systems exist for CP, with the traditional aspects based on seven different axes: physiological (type/nature of motor or movement disorder), topology, supplemental, etiologic, neuroanatomic (radiologic), therapeutic and functional (101). Here, we discuss the most widely used, first two classification categories.

Physiologic classification involves the type and nature of motor or movement disorder (the quality and change in muscle tone). The most commonly defined subtype is *spastic CP* (characterized mainly by muscle hypertonia), seen in 72-91% of cases, pathophysiological described by dysfunction of the inhibitory interneurons of the

corticospinal tract (102). The second most frequent form is *dyskinetic (or athetoid) CP*, further divided into *dystonic* and *choreo-athetoid*, which are caused by injury to the thalamus and basal ganglia. This subtype is seen in 15% of children with CP, characterized by uncoordinated movements of the upper and lower limb together with abnormal posture (103). The rarest form is *ataxic CP*, involving generalized muscle hypotonia together with loss of muscle coordination (presumably suggesting cerebellar injury), described in 4-5% of cases (104). The remaining cases constitute *mixed type CP*, characterized by a mixture of the upper described symptoms (105). Previously, *hypotonic CP* has been separately differentiated; however, recent evidence demonstrated that hypotonic cases are either mild forms of ataxic CP, or merely transient forms, where the leading motor dysfunction (usually spasticity of the extremities) has not appeared yet (102). This emphasizes the importance of well-timed diagnosis and classification, which is reliable starting from 3-4 years of age, and requiring regular follow-up into the adolescent years (105).

Topological classification of CP is done in case of spastic subtype of CP, based on the guidelines of the Surveillance of Cerebral Palsy in Europe (SCPE) collaboration (102). This system divides localization into unilateral and bilateral CP:

- Unilateral palsy includes
 - *monoplegia*, where only one limb is affected (usually being the lower limb), and
 - *hemiplegia*, affecting one half of the body (with usually the upper limb being the more severely affected).
- Bilateral palsy can be further categorized into
 - *diplegia*, all limbs are affected (but the upper limbs only show fine motor impairment),
 - *triplegia*, with the typical pattern of one affected upper limb and bilateral (asymmetric) lower limb involvement, and
 - *tetraplegia*, where all four limbs and the trunk is also affected.

Nevertheless, the observed CP type is rarely permanent, as progression of the disease includes change of the most prominent muscle tone dysfunction and limb involvement (104).

1.4.2.2 Functional severity

A number of functional classification systems exist for CP severity, with the most widely used being the Gross Motor Function Classification System (GMFCS), the Manual Ability Classification System (MACS), the Communication Function Classification System (CFCS), and the Eating and Drinking Ability Classification System (EDACS). These have the advantage of grading CP severity by degree of caused functional disability, and can thus accurately monitor progression or response to therapy (106).

In Hungary, the adapted version of GMFCS is applied, which scores the degree of caused disability on a five-level scale, from I to V, and accurately quantifies functional severity (107). The GMFCS scores are presented in *Table 3*.

1.4.2.3 Management and prognosis

To date, no definitive treatment exists for CP, thus the mainstream for reducing the incidence and health impact of this disease is effective prevention (i.e. pre- and perinatal maternal and infant care to overcome risk factors), as well as close follow-up and management (108). The later include motor (i.e. physiotherapy and kinesiology), as well as occupational rehabilitation, aiming at improving critical thinking, self-sufficiency and problem solving. Neurorehabilitation is also provided, if needed, targeting the reduction of spasticity using baclofen or botulinum toxin A, and in refractive cases, surgical interventions like selective rhizotomy or neurotomies (105).

Due to the increasing scope of rehabilitation and care, the average life expectancy of patients with CP is constantly increasing. As a result of better nutrition, more aggressive prevention and cure of infections and improving surgical techniques, 50% of even the most severely affected children will survive into the middle of their third decade (97). This is a welcoming result, as long as the increased years of survival are spent in good life quality. To guarantee the improving life conditions of patients affected with CP, knowledge of regional CP risk factors, prevalence and severity is vital, to assess where improvement of interdisciplinary management is needed. This underscores the need for a national Hungarian registry, to monitor CP prevalence and optimize follow-up.

Table 3. The Gross Motor Function Classification System (GMFCS).

Categories showing capabilities and situations causing disability. Adapted for children aged 6 to 12 years (107).

<p>GMFCS Level I</p>	<ul style="list-style-type: none"> - walk at home, school, outdoors and in the community, - can climb stairs without the use of a railing, - perform gross motor skills such as running and jumping, - speed, balance and coordination are limited.
<p>GMFCS Level II</p>	<ul style="list-style-type: none"> - walk in most settings and climb stairs holding onto a railing, - may experience difficulty walking long distances and balancing on uneven terrain, inclines, in crowded areas or confined spaces, - may walk with physical assistance, a handheld mobility device or wheeled mobility over long distances, - have only minimal ability to perform gross motor skills such as running and jumping.
<p>GMFCS Level III</p>	<ul style="list-style-type: none"> - walk using a hand-held mobility device in most indoor settings, - may climb stairs holding onto a railing with supervision or assistance, - use wheeled mobility when traveling long distances, and may self-propel for shorter distances.
<p>GMFCS Level IV</p>	<ul style="list-style-type: none"> - use methods of mobility that require physical assistance or powered mobility in most settings, - may walk for short distances at home with physical assistance or use powered mobility or a body support walker when positioned, - at school, outdoors and in the community children are transported in a manual wheelchair or use powered mobility.
<p>GMFCS Level V</p>	<ul style="list-style-type: none"> - are transported in a manual wheelchair in all settings, - are limited in their ability to maintain antigravity head and trunk postures and control leg and arm movements.

2 Objectives

In the research projects constituting the basis for my doctoral dissertation, I examined the prognostic utility and optimization possibilities of conventionally acquired brain H-MRS to predict long-term outcome in newborns with moderate-to-severe HIE. Moreover, I assessed the prevalence, clinical manifestation and severity of CP diagnosed following PA/HIE. During my research, my principal questions were as follows:

2.1 Predictive value of early, conventional brain H-MRS in neonatal HIE

- a. Is early (first 96 postnatal hours), conventional brain H-MRS suitable for prediction of long-term neurodevelopmental outcome in newborns with HIE?
- b. Which brain metabolite ratios show strong association with outcome?
- c. How do these metabolite ratios correlate with postnatal age at scan, in the first 96 postnatal hours?
- d. What is the predictive value, sensitivity and specificity of the metabolite ratios showing weak or no correlation with postnatal age at scan?

2.2 Optimal postnatal age at H-MRS for outcome prediction in newborns with HIE

- a. How does predictive value of brain H-MRS change with postnatal age during the first two weeks of life in newborns with HIE?
- b. Is brain H-MRS suitable for outcome prediction throughout the first 14 postnatal days, irrespective of postnatal age at scan?
- c. Which postnatal age period provides the highest predictive accuracy?

2.3 Dynamic changes of brain H-MRS metabolite ratios in neonatal HIE

- a. Does gestational age and postnatal age at scan affect the measured brain H-MRS metabolite ratios overall, during the first 14 days of life in newborns with HIE?
- b. How are metabolite ratios associated with gestational age and postnatal age, when analyzed separately based on neurological outcome?

2.4 Prevalence and clinical manifestation of CP at Semmelweis University

- a. What is the prevalence of PA/HIE among children diagnosed with CP at the clinics of Semmelweis University?
- b. What clinical manifestation and severity can be observed in children with post-asphyxial/post-hypoxic-ischemic CP at the examined clinics?
- c. Does the observed prevalence and clinical presentation differ from those reported from existing CP registers?

3 Methods

3.1 Patient selection

3.1.1 Predictive value of early, conventional H-MRS in neonatal HIE

In our 1st, retrospective descriptive analysis, we reviewed all 283 patients born between January 2006 and December 2010 and admitted with suspected HIE to the regional cooling center, the Neonatal Intensive Care Unit (NICU) of the 1st Department of Paediatrics, Semmelweis University, Budapest, Hungary. Selection of newborns with suspected HIE was done according to the admission log.

From this patient pool, we included in our study all patients who (A) fulfilled the diagnostic criteria for moderate-to-severe HIE, based on the international TOBY trial (27), described in detail in chapter 1.1.3, AND (B) underwent a brain H-MRS examination before the 96th postnatal hour; AND (C) had a neurodevelopmental follow-up result, as detailed in chapter 3.4.

From this patient pool, we excluded all newborns who (d) had other underlying conditions which could cause encephalopathy besides HIE (i.e. stroke, intracranial hemorrhage, congenital malformation or metabolic disease). Considering that at the time of the study, only early onset (< 6 postnatal hours) HT was thought to be effective for neuroprotection, we excluded patients who (e) did not receive HT due to delayed admission. Further exclusion criteria were: (f) gestational age < 36 weeks and (g) low quality brain H-MRS.

Altogether, 51 patients met all the criteria and were included in the analysis (see *Figure 4.*).

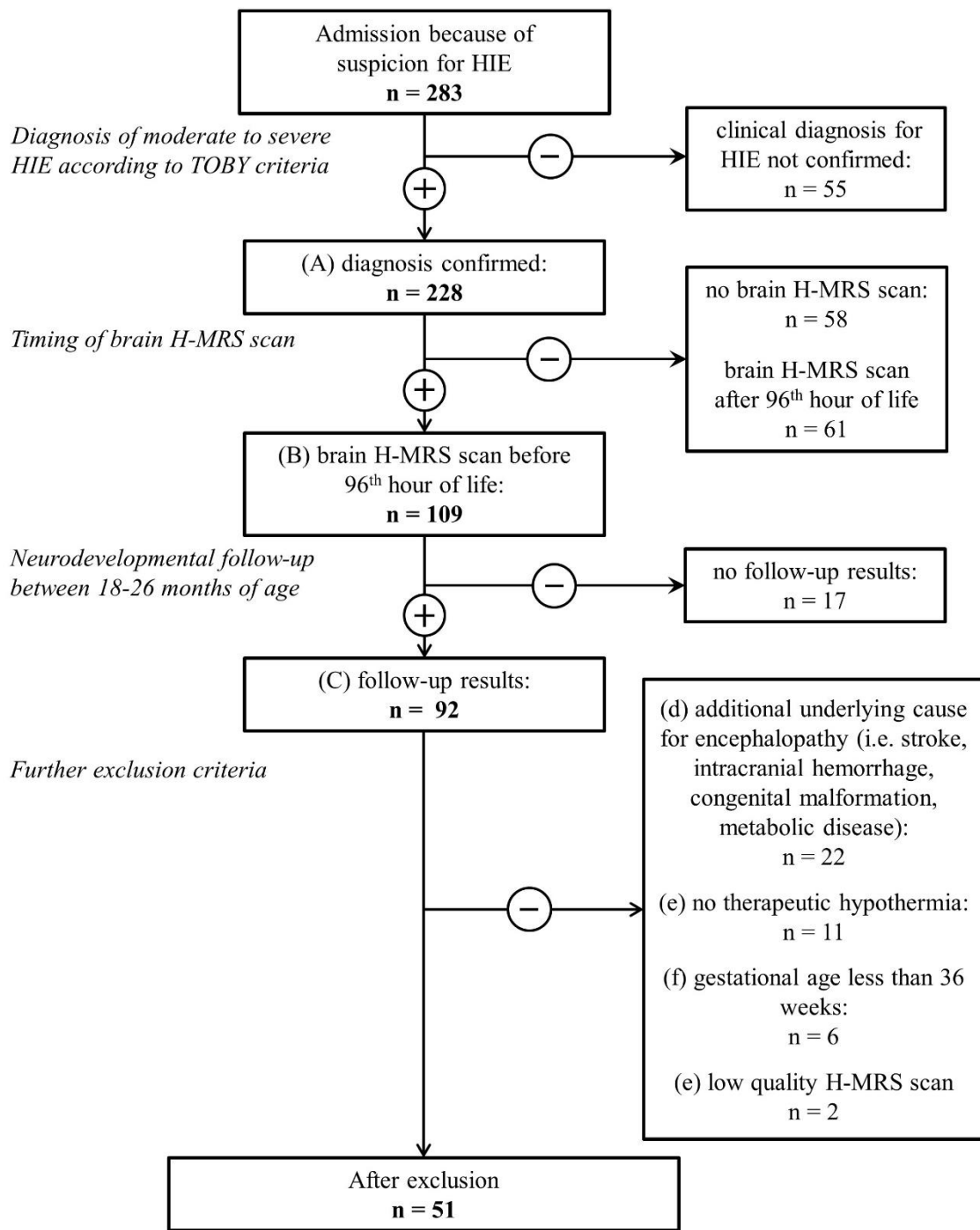


Figure 4. Algorithm for patient selection in our 1st study, analyzing predictive utility of early (first 96 hours), conventional H-MRS in newborns with HIE.

3.1.2 Optimal postnatal age at H-MRS for outcome prediction in HIE

For our 2nd retrospective analysis, we reviewed all 484 newborns admitted to our NICU between 2006 and 2016 with confirmed moderate-to-severe HIE (according to the TOBY criteria (27)).

From this patient pool, we included in our investigation neonates who (A) had a H-MRS examination in the first 14 days of life (DOL), and (B) had a neurodevelopmental follow-up result, as detailed in chapter 3.4.

From the newborns eligible to the inclusion criteria, we excluded those who (c) were born at < 36 gestational weeks, and (d) had other etiologies for encephalopathy besides HIE (i.e. stroke, intracranial hemorrhage, metabolic disease or congenital malformation). Inclusion and exclusion criteria are presented in detail in *Figure 5*.

Next, we divided the newborns into three categories, based on postnatal age at first performed H-MRS examination (where more than one was done during the first 2 weeks of life):

- early H-MRS (DOL 1-3), indicating the common time period for the gold standard HT (27),
- midtime H-MRS (DOL 4-6) and
- late H-MRS (DOL \geq 7), the recommended time for a control MR examination, according to guidelines (44).

3.1.3 Dynamic changes of H-MRS metabolite ratios in neonatal HIE

The inclusion and exclusion criteria of our 3rd analysis was identical to the one examined in our 2nd study, conclusively, we enrolled newborns with moderate-to-severe HIE, having at least one H-MRS examination during the first 14 postnatal days, as well as known neurodevelopmental outcome, as described in detail in chapter 3.4. Patient selection is presented in *Figure 5*.

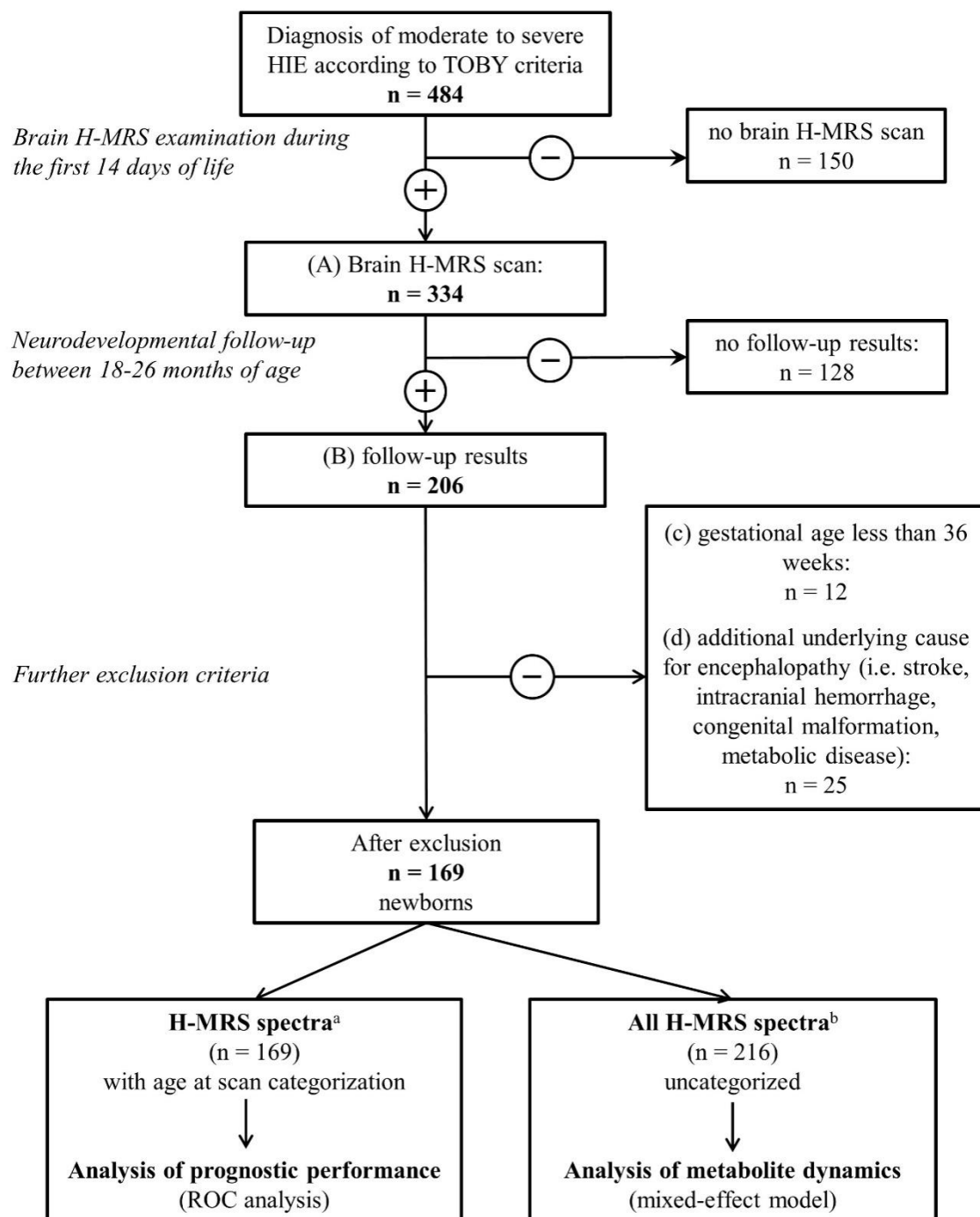


Figure 5. Algorithm for patient selection in our 2nd and 3rd study, analyzing optimal postnatal age at scan and metabolite dynamics for H-MRS, in newborns with HIE.

^a Age at scan categorization was done based on the initial (1st) performed H-MRS, where more than one H-MRS scan was performed

^b Initial (1st) and repeated (2nd and 3rd) H-MRS results were also included, without age at scan categorization

ROC: Receiver-Operating Characteristics.

For analysis of metabolite dynamics, we included all performed H-MRS examinations of enrolled infants: the ones included in the previous analysis (i.e. first scans), as well as the repeated examination(s), where applicable (i.e. second and third scans). The results of these examinations were analyzed irrespective of the postnatal age categories described in chapter 3.1.2.

3.1.4 Prevalence and clinical presentation of CP at Semmelweis University

In our 4th retrospective pilot study, we reviewed patient records of all children born between 2005 January - 2015 December, and diagnosed or treated with CP at the departments of Semmelweis University enrolled in the routine care of CP: 1st Department and 2nd Department of Paediatrics, as well as Department of Orthopaedics, Semmelweis University, Budapest. Patient data of eligible children were collected using International Classification of Diseases (ICD) codes applied for diagnosis of CP, as determined by orthopedic surgeons, being as follows:

- G8000: Spastic cerebral palsy,
- G8010: Spastic bilateral palsy,
- G8030: Dyskinetic cerebral palsy,
- G8040: Ataxic cerebral palsy,
- G8090: Infantile cerebral palsy, not otherwise specified,
- G8110: Unilateral spastic palsy,
- G8190: Unilateral palsy, not otherwise specified,
- G8240: Spastic tetraplegia,
- G8250: Tetraplegia, not otherwise specified,
- M6240: Muscle contracture, not otherwise specified.

We included in our analysis all children with confirmed diagnosis of CP, based on thorough revision of available patient documentation in the Semmelweis University's electronic patient record system MedSolution. Children where the relevant ICD codes were registered due to suspicion or preliminary, but later unconfirmed CP diagnosis were excluded from further analysis.

Next, we reviewed the available patient history to determine the possible risk factors that could be linked to CP. Finally, we performed the clinical and topological classification of CP cases, as well as severity assessment using the GMFCS scale, as detailed in chapter 1.4.2.2.

3.2 Clinical care of newborns with HIE

According to the local NICU protocol, whole-body HT was initiated in each case fulfilling the therapeutic criteria as established by the TOBY trial (27). Cooling was started as soon as possible, but within 6 hours after delivery (or in case of postpartum asphyxia, after the hypoxic-ischemic insult), using a water-filled mattress (Tecotherm©; TecCom, Halle, Germany). The target rectal temperature was between 33 and 34 °C, which was maintained for 72 hours. In the rewarming phase, temperature increase velocity was 0.5 °C/h. All newborns were ventilated throughout the cooling and rewarming phase.

A loading dose of morphine (0.1 mg/kg BW) was administered as soon as HT was initiated, followed by continuous morphine sedation (10 µg/kg BW/h), in order to alleviate the discomfort of hypothermia as well as to prevent shivering (31). If clinical or electrophysiological seizures were detected, anticonvulsant therapy was provided, with phenobarbitone (loading dose 20 mg/kg) as first line therapy. In case of noncontrolled seizures, the phenobarbitone loading dose was repeated, or midazolam was given in single or repeated doses (0.1 mg/kg BW), or in continuous infusion (0.1 mg/kg BW/h). In some cases, newborns with therapy resistant convulsions received phenytoin or diazepam or chloral hydrate, as a third line choice treatment, according to the attending clinician's decision. All infants were monitored by continuous aEEG for a minimum of 96 hours or until trace normalization.

3.3 Brain H-MRS examination

Brain H-MRS examination was performed as part of brain MR examination, which is the routine diagnostic imaging for newborns with HIE in our unit as a center practice. The scans were carried out on a 3 Tesla Philips Achieva MRI scanner between 2006-2015, and on a 3 Tesla Philips Ingenia MRI scanner in 2016 (Philips Medical Systems, Best,

The Netherlands), at the Department of Neuroradiology of the Medical Imaging Center, Semmelweis University, as soon as the infants reached clinical stability and were suitable for transport. The Neonatal Emergency & Transport Services of the Peter Cerny Foundation provided the newborns' transport. NICU medical staff of the 1st Department of Paediatrics provided analgesia, ventilation, HT and medical supervision during scan. For the time of the MR examination, newborns were removed from the incubator, and received continuous morphine sedation. In case of intubated neonates, manual ventilation was provided by skilled personnel, using an AMBU bag. Throughout the examination, all infants underwent continuous monitoring of pulse and transcutaneous oxygen saturation (Medrad Veris MR Monitoring System, Bayer Healthcare LLC, Whippany, NJ).

Proton MR spectra were acquired using PRESS (Point RE-Solved Spectroscopy) single voxel localization sequence, with a repetition time (TR) of 2000, number of acquisitions 128, on three different TEs: 35 ms, 144 ms and 288 ms. The analyzed VOI was a 1 x 1 x 1 cm (1 cm³) voxel from the left thalamus of the infants, localized based on gradient echo survey images acquired with TE = 5 ms, TR = 75 ms and 30° flipangle.

3.3.1 Metabolites and metabolite ratios

From the acquired H-MRS, we registered the most frequently analyzed metabolites, being as follows: NAA, Cho, Cr, mI and Lac. Physiological and pathological function, as well as TE-dependent acquisition of these metabolites is described in detail in chapter 1.3.1. From the registered spectrum, we measured and recorded each metabolite curve's peak height and peak area.

3.3.2 H-MRS analysis

To ensure generalizability of the obtained results, we only used the vendor-provided data-processing software of the MR console for analysis, without any specific equipment or tool for data-optimization. Our aim was to reproduce basic, non-research center hospital level circumstances, therefore, no data-optimizing equipment or further post-processing methods were used to improve the registered spectra. To ameliorate the precision of our analysis, we excluded metabolite curves – and thus the metabolite ratios derived from

them –, which could only be acquired with extreme high noise level (i.e. with signal-to-noise ratio (SNR) < 2).

We did not use absolute quantification protocols due to their high technical requirements, consequently, statistical analysis was carried out on ratios of peak heights and ratios of peak areas, recorded at same TE.

3.3.3 Predictive value of early, conventional brain H-MRS in neonatal HIE

For our 1st study, our initial approach was a hypothesis-free, data-driven analysis, to determine whether conventional brain H-MRS during the first 96 hours of life is suitable for outcome prediction in newborns with HIE. Consequently, we analyzed all 36, routinely measured metabolite ratios of peak heights and ratios of peak areas, listed in *Table 4*.

Table 4. List of ratios of peak heights, and ratios of peak areas of the analyzed metabolites.

NAA: N-acetyl-aspartate, Cho: choline, Cr: creatine, mI: myo-inositol, Lac: lactate, TE: echo time. Metabolite spectra were determined at TEs 35 ms, 144 ms and 288 ms.

TE = 35 ms	TE = 144 ms	TE = 288 ms
• NAA/Cho height	• NAA/Cho height	• NAA/Cho height
• NAA/Cho area	• NAA/Cho area	• NAA/Cho area
• NAA/Cr height	• NAA/Cr height	• NAA/Cr height
• NAA/Cr area	• NAA/Cr area	• NAA/Cr area
• Cho/Cr height	• Cho/Cr height	• Cho/Cr height
• Cho/Cr area	• Cho/Cr area	• Cho/Cr area
• mI/NAA height	• mI/NAA height	• Lac/NAA height
• mI/NAA area	• mI/NAA area	• Lac/NAA area
• mI/Cho height	• mI/Cho height	• Lac/Cho height
• mI/Cho area	• mI/Cho area	• Lac/Cho area
• mI/Cr height	• mI/Cr height	• Lac/Cr height
• mI/Cr area	• mI/Cr area	• Lac/Cr area

3.3.4 Optimal postnatal age at H-MRS for outcome prediction in HIE

For our 2nd study, we concentrated our analysis on the metabolite ratios showing the highest predictive value based on existing research and our previous study. We focused on TE = 144 ms spectra, seeing that it provides adequate compromise between the determined number of metabolites and level of noise, furthermore, it is the most commonly used TE setting for brain H-MRS in newborns with HIE. The metabolite ratios included in the 2nd analysis are:

- NAA/Cho height
- NAA/Cho area
- NAA/Cr height
- NAA/Cr area
- mI/NAA height
- mI/NAA area

3.3.5 Dynamic changes of H-MRS metabolite ratios in neonatal HIE

In our 3rd analysis, we included the metabolite ratio/ratios that showed high predictive value throughout the examined first 14 days of life of newborns with HIE, across all three postnatal age categories, based on the results of our 2nd analysis.

3.4 Neurodevelopmental outcome

Neurodevelopmental follow-up is routinely measured between 18-26 months of age, using the Bayley Scales of Infant Development II tool-kit (95), by trained personnel (either a trained pediatrician or child psychologist), blinded to the H-MRS results. Details on the Bayley II test are presented in chapter 1.4.1.

For our studies, we defined poor outcome as either death (< 28 days of age or > 28 days associated with HIE) OR moderately/severely delayed development on either the mental or the psychomotor scale (MDI or PDI < 70) OR diagnosis of cerebral palsy, hearing loss or visual loss. All other outcomes (MDI and PDI both \geq 70) were considered as good outcome.

3.5 Statistical analysis

Categorical variables are presented as sample size (n) and percentage (%), while continuous variables are reported as mean \pm standard deviation or median [25th to 75th interquartile range], depending on the distribution of the parameters. Normality was assessed using Shapiro-Wilk test. Categorical variables were compared with the Fisher's exact test or chi-squared test (X^2), while continuous variables were compared with the Student t-test or Mann-Whitney U-test, for parametric and non-parametric comparisons, respectively. Generally, we considered statistical tests to be significant at $p < 0.05$.

Demographic, clinical and spectral data were analyzed and plotted using GraphPad Prism 7.0, IBM SPSS Statistics 23.0 as well as R Statistical software 4.0.2.

3.5.1 *Predictive value of early, conventional brain H-MRS in neonatal HIE*

In the 1st study, we used Mann-Whitney U-test to select metabolite ratios showing significant association with outcome. As it has been described that brain metabolism undergoes intense postnatal age dependent alterations following the hypoxic insult, we aimed to search and select for the exceptions, namely those metabolite ratios that show weak or no correlation with postnatal age, and would thus be suitable for prognosis any time during the analyzed first 4 postnatal days. Postnatal age dependence of metabolite ratios was assessed using Spearman rank-correlation test. Next, we used Receiver-Operating Characteristics (ROC) analysis to assess the predictive value of metabolite ratios associated with outcome, and showing weak or no correlation with postnatal age. Finally, we compared the metabolite ratios as diagnostic tests using the area-under-the-ROC curve (AUC), using the method described by Hanley and McNeil (109).

Due to the high number of analyzed metabolite ratios and comparisons, we used Bonferroni-correction to overcome the problem of multiple testing. Conclusively, due to 36 examined metabolite ratios, we considered statistical results significant at $p < 0.0014$ ($0.05/36 = 0.0014$) in all analyses of the 1st study.

3.5.2 Optimal postnatal age at H-MRS for outcome prediction in neonatal HIE

In the 2nd study, we extended our research concept described previously, and tested predictive accuracy of H-MRS in postnatal age windows beyond the 4th day of life. For this, the metabolite ratios' association with outcome was determined separately in the three postnatal age category groups (early, midtime and late), using Mann-Whitney U-test. We selected metabolite ratios showing significant association with outcome throughout all three age categories, and assessed predictive value using ROC analysis.

3.5.3 Dynamic changes of H-MRS metabolite ratios in neonatal HIE

In our 3rd study, we aimed to refine the earlier results for a more precise prediction. To this end, metabolite ratios showing strong association with outcome, throughout all three examined postnatal age categories, were included in a repeated-measures linear mixed-effect regression model, with first-order autoregressive within-group correlation structure fitted by maximizing the restricted log-likelihood, in order to assess metabolite dynamics. The dependent variables for the regression model were the metabolite ratios, covariates were: gestational age (weeks), postnatal age (days) and poor outcome. The mixed-effect model was constructed generally, in the whole population, and separately in the two outcome groups, as well.

3.5.4 Prevalence and clinical presentation of CP at Semmelweis University

In our 4th study, prevalence of different clinical presentations was presented using sample size (n) and percentage (%). The prevalence values registered among CP cases following perinatal asphyxia/hypoxic-ischemic encephalopathy (post-PA CP) were compared to overall prevalence values using Fisher's exact test and X^2 test.

3.6 Ethical considerations

Ethical permission for the 1st, 2nd and 3rd analyses was obtained from the Scientific and Medical Research Council Ethics Committee of Hungary (11790-2/2016/EKU). The infants enrolled did not undergo any procedures or interventions solely for the purposes of the studies. Both brain MRI and H-MRS, as well as neurodevelopmental follow-up examinations are part of the routine imaging and diagnostic protocol of our unit, and are

performed on all newborns with suspected moderate-to-severe HIE. The use of these imaging tools help the clinician confirm the diagnosis, determine the timing and nature of the hypoxic-ischemic insult (chronic intrauterine or intrapartum), as well as rule out other etiologies.

As our 4th study was a pilot audit investigation, to assess patient documentation quality as well as prevalence and clinical manifestation of CP cases, no ethical permission was needed.

4 Results

4.1 Predictive value of early, conventional brain H-MRS in neonatal HIE

After our patient selection described in detail in chapter 3.1.1, 51 newborns with moderate-to-severe HIE were enrolled in the study. HT was initiated before the 6th postnatal hour for all 51 neonates, at median [IQR] 2 [1.4; 3.1] hours. Forty-five out of the 51 patients had the H-MRS examination done while receiving HT. The remaining 6 patients had the examination performed before the initiation, or after the completion of HT. Nevertheless, all scans were performed within 96 hours of age, with the earliest scan done at 5 hours of age.

Clinical characteristics of these 51 neonates are presented in *Table 5*, categorized by long-term outcome. Of the 16 patients considered to have poor outcome, 9 infants died. Of these 16 patients, 7 patients survived but had moderately/severely delayed development based on either the mental or the psychomotor scale determined using the Bayley II test (either MDI or PDI < 70), 4 infants were diagnosed with CP (2 associated with mental retardation and one with epilepsy), 2 had mental retardation, and one patient suffered from neuronal hearing loss and epilepsy. As presented in *Table 5*, good and poor outcome groups only differed significantly in their 5 min and 10 min Apgar scores.

MRI findings of these 51 infants are presented in *Table 6*, categorized by outcome. The outcome groups did not differ significantly in the occurrence of abnormalities seen on MRI images < 96 postnatal hours.

Analysis of the metabolite ratios' association with long-term outcome revealed that out of the examined 36 metabolite ratios, only 3 metabolite ratios were able to significantly ($p < 0.0014$, after Bonferroni-correction) differentiate between good and poor outcome, in the first 96 hours of newborns: mI/Cr height (TE = 35 ms, $p = 0.0005$), mI/NAA height (TE = 35 ms, $p < 0.0001$) and NAA/Cr height (TE = 144 ms, $p < 0.0001$). Further results of the Mann-Whitney U-test, as well as results of the 33 metabolite ratios not significantly ($p > 0.0014$) associated with outcome, are presented in *Table 7*.

Table 5. Clinical characteristics of newborns enrolled in the study (n = 51).

Data shown as median [IQR], mean \pm SD or percentage.

Good outcome is defined as both MDI and PDI \geq 70 achieved on Bayley II test, poor outcome is defined as either MDI or PDI $<$ 70 OR death ($<$ 28 days of age OR $>$ 28 days of age associated with HIE).

BD: base deficit, aEEG: amplitude-integrated electroencephalography, CNV: continuous normal voltage, DNV: discontinuous normal voltage, BS: burst suppression, LV: low voltage, FT: flat trace, MR: magnetic resonance, DWI: diffusion weighted imaging.

* represents significant results surviving Bonferroni-correction ($p < 0.0014$).

NA (not applicable) represents statistical significance not applicable as death was included in the definition of the poor outcome group.

Variable	Good outcome (n = 35)	Poor outcome (n = 16)	p value
Male sex	19 (51%)	12 (75%)	0.1365
Gestational age (weeks)	39 [38; 40]	38 [37; 40]	0.0536
Birth weight (g)	3261 \pm 577	3128 \pm 537	0.4379
Apgar 1'	2 [1; 4]	1 [0; 2]	0.0091
Apgar 5'	5 [4; 7]	3 [2; 4]	0.0002*
Apgar 10'	6 [5; 8]	4 [2; 4]	0.0005*
Lowest pH $<$ 1hour of age	7.21 [6.98; 7.28]	7.10 [7.00; 7.20]	0.1643
Highest BD $<$ 1hour of age	14.1 \pm 5.9	17.1 \pm 4.6	0.0860
Onset of hypothermia (h)	1.8 [1.4; 3.1]	2.1 [1.4; 3.3]	0.6309
Clinical or aEEG seizures ($<$ 24 h)	28 (80%)	14 (88%)	0.7012
Abnormal aEEG pattern (BS, LV, FT)	31 (88%)	12 (75%)	0.2396
aEEG normalization (CNV, DNV) $<$ 72 h	22 (63%)	5 (31%)	0.0681
aEEG normalization time (h)	30 [12; 47]	60 [42; 68]	0.1381
Age at MR scan (h)	25 [14; 49]	30 [16; 54]	0.6625
Abnormalities on MR imaging (T1/T2 weighted imaging or DWI)	13 (37%)	11 (69%)	0.0681
Death	0	9 (56%)	NA

Table 6. Location and severity of observed magnetic resonance imaging (MRI) abnormalities in newborns with good versus poor outcome.

Abnormalities are described as signal intensity abnormality on T1/T2 weighted images, or diffusion abnormality.

* represents significant results surviving Bonferroni-correction ($p < 0.0014$).

	MRI abnormality and good outcome (n = 13)	MRI abnormality and poor outcome (n = 11)	p value
Location of injury			
<i>Basal ganglia and thalami</i>	6 (46%)	8 (72%)	0.2397
<i>Internal capsule</i>	5 (38%)	6 (54%)	0.6824
<i>White matter</i>	5 (38%)	0 (0%)	0.0411
<i>Cortex</i>	1 (8%)	1 (9%)	>0.9999

Table 7. Results of Mann-Whitney U-test, assessing association between metabolite ratios and long-term outcome.

NAA: N-acetyl-aspartate, Cr: creatine, TE: echo time, Cho: choline, mI: myo-inositol, Lac: lactate.

* represents significant results ($p < 0.0014$), also emphasized by bold font.

Assessed metabolite ratio	value of metabolite ratio (median [IQR])		p value
	good outcome (n=35)	poor outcome (n=16)	
NAA/Cr height (TE = 35 ms)	0.8671 [0.8183; 0.9658]	0.8183 [0.6436; 0.8573]	0.0288
NAA/Cr area (TE = 35 ms)	0.9590 [0.8889; 1.110]	0.8453 [0.7146; 1.010]	0.0946
NAA/Cho height (TE = 35 ms)	1.003 [0.8859; 1.201]	1.064 [0.8448; 1.143]	0.7669
NAA/Cho area (TE = 35 ms)	0.9717 [0.8037; 1.078]	0.8481 [0.7599; 1.021]	0.3374
Cho/Cr height (TE = 35 ms)	0.8285 [0.7738; 0.9534]	0.8365 [0.6604; 0.9699]	0.5656
Cho/Cr area (TE = 35 ms)	1.005 [0.9394; 1.156]	0.9168 [0.7779; 1.230]	0.2143
mI/Cr height (TE = 35 ms)	0.4706 [0.3867; 0.5297]	0.6402 [0.5277; 0.7241]	0.0005*
mI/Cr area (TE = 35 ms)	0.8682 [0.6645; 0.9688]	1.092 [0.7907; 1.340]	0.0595
mI/NAA height (TE = 35 ms)	0.5337 [0.4402; 0.6104]	0.7804 [0.6937; 0.8939]	<0.0001*
mI/NAA area (TE = 35 ms)	0.8725 [0.6758; 1.024]	1.179 [1.098; 1.371]	0.0057
mI/Cho height (TE = 35 ms)	0.4865 [0.4298; 0.6420]	0.7905 [0.5385; 0.8775]	0.0027
mI/Cho area (TE = 35 ms)	0.7869 [0.6197; 0.9446]	1.000 [0.7978; 1.286]	0.0223
NAA/Cr height (TE = 144 ms)	0.9900 [0.8974; 1.096]	0.8082 [0.6897; 0.8630]	<0.0001*
NAA/Cr area (TE = 144 ms)	0.9541 [0.8744; 1.085]	0.8350 [0.7529; 0.9147]	0.0050
NAA/Cho height (TE = 144 ms)	0.92654 [0.7326; 1.062]	0.7761 [0.6004; 0.9041]	0.0418
NAA/Cho area (TE = 144 ms)	0.6708 [0.5916; 0.7639]	0.5922 [0.5258; 0.6978]	0.0552
Cho/Cr height (TE = 144 ms)	1.103 [0.9743; 1.302]	1.022 [0.8516; 1.359]	0.2389
Cho/Cr area (TE = 144 ms)	1.473 [1.348; 1.605]	1.320 [1.271; 1.470]	0.0877

Table 7 (continued). Results of Mann-Whitney U-test, assessing association between metabolite ratios and long-term outcome. * represents significant results ($p < 0.0014$), also emphasized by bold font.

Assessed metabolite ratio	value of metabolite ratio (median [IQR])		p value
	good outcome (n=35)	poor outcome (n=16)	
mI/Cr height (TE = 144 ms)	0.3979 [0.3196; 0.4976]	0.4066 [0.3717; 0.4615]	0.5777
mI/Cr area (TE = 144 ms)	0.6271 [0.4615; 0.8844]	0.7763 [0.5986; 0.9557]	0.2598
mI/NAA height (TE = 144 ms)	0.3872 [0.3314; 0.4950]	0.5336 [0.4592; 0.5953]	0.0114
mI/NAA area (TE = 144 ms)	0.6417 [0.4716; 0.8770]	0.8910 [0.7957; 1.090]	0.0162
mI/Cho height (TE = 144 ms)	0.3497 [0.3054; 0.4080]	0.4284 [0.3445; 0.5401]	0.1433
mI/Cho area (TE = 144 ms)	0.4088 [0.3480; 0.5588]	0.5718 [0.4576; 0.7106]	0.0503
NAA/Cr height (TE = 288 ms)	1.395 [1.128; 1.506]	1.191 [0.9924; 1.259]	0.1047
NAA/Cr area (TE = 288 ms)	1.423 [1.149; 1.619]	1.463 [1.126; 1.543]	0.9825
NAA/Cho height (TE = 288 ms)	0.9609 [0.7782; 1.103]	0.8192 [0.6838; 0.8759]	0.0667
NAA/Cho area (TE = 288 ms)	0.8384 [0.7383; 0.9555]	0.8116 [0.6767; 1.068]	0.9400
Cho/Cr height (TE = 288 ms)	1.428 [1.225; 1.622]	1.360 [1.076; 1.972]	0.8896
Cho/Cr area (TE = 288 ms)	1.633 [1.443; 1.966]	1.632 [1.500; 2.075]	0.8865
Lac/Cr height (TE = 288 ms)	0.1877 [0.1546; 0.2283]	0.3289 [0.2619; 0.6619]	0.0059
Lac/Cr area (TE = 288 ms)	0.4206 [0.3127; 0.5072]	0.9143 [0.7500; 1.238]	0.0037
Lac/Cho height (TE = 288 ms)	0.1479 [0.1169; 0.1883]	0.2599 [0.1494; 0.3475]	0.0289
Lac/Cho area (TE = 288 ms)	0.2469 [0.2098; 0.3589]	0.6444 [0.3001; 0.7439]	0.0059
Lac/NAA height (TE = 288 ms)	0.1484 [0.1167; 0.2629]	0.2967 [0.2731; 0.5493]	0.0205
Lac/NAA area (TE = 288 ms)	0.2994 [0.2281; 0.4713]	0.5926 [0.5488; 1.099]	0.0093

As seen in *Figure 6*, the poor outcome group showed significantly higher mI/Cr and mI/NAA ratios, as well as lower NAA/Cr ratio, compared with the good outcome group, thus these metabolite ratios can accurately differentiate between outcome groups.

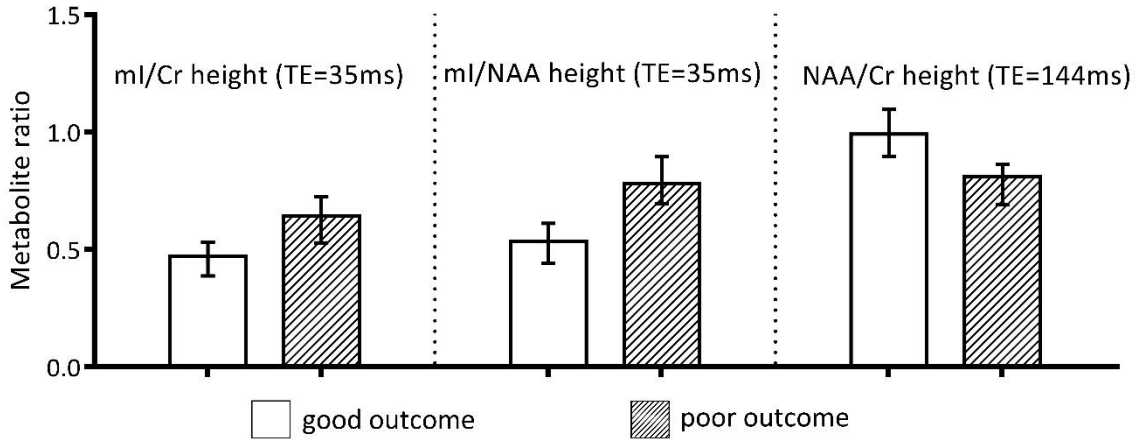


Figure 6. Metabolite ratios significantly associated with outcome, as detected in newborns with HIE facing good and poor outcome

Bars represent median and interquartile range values, the corresponding exact p values are presented in *Table 7*.

Next, we assessed the postnatal age dependence of these 3 metabolite ratios among all 51 patients, during the first 96 postnatal hours. Neither mI/Cr, nor mI/NAA or NAA/Cr ratios were correlated with postnatal age at scan, based on p values of Spearman rank correlation ($p = 0.878, 0.384$ and 0.056 , respectively), hence might be considered stable during the first 96 postnatal hours. Plots and results of Spearman rank correlation are presented on *Figure 7*.

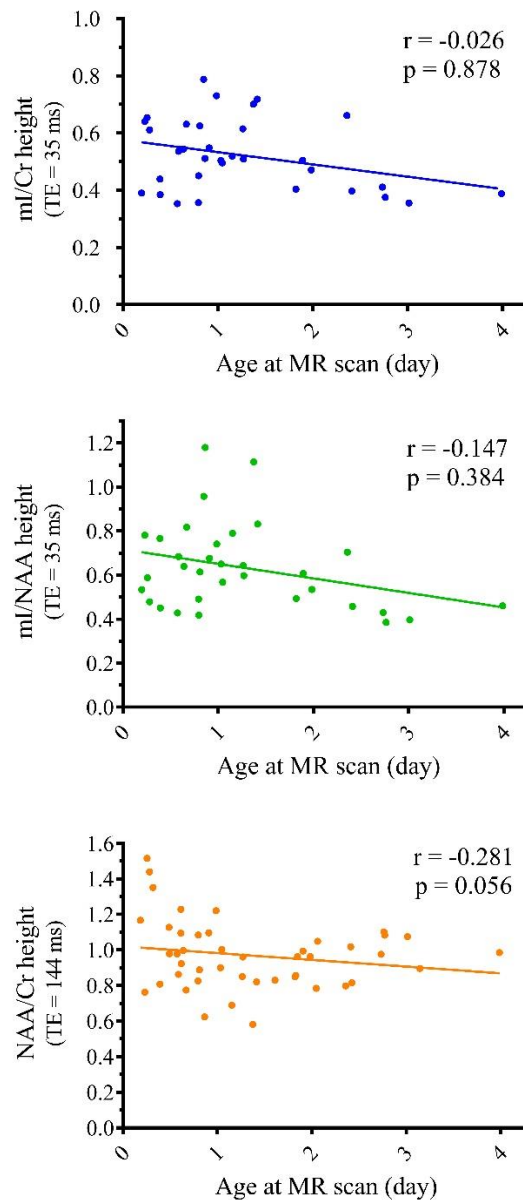


Figure 7. Age-correlation diagrams of the 3 metabolite ratios showing strong association with outcome.

r: Spearman rank correlation coefficient.

Finally, ROC analysis concluded that out of these 3 age-independent metabolite ratios, mI/NAA height had a stronger discriminative power than mI/Cr height and NAA/Cr height, to differentiate between infants facing good and poor outcome (cut-off values 0.6798, 0.6274 and 0.7798, respectively, AUC: 0.9084, 0.8462 and 0.8396, respectively, difference between ROC curves $p < 0.0001$, according to Hanley & McNeil's method (109)). Conclusively, out of the 36 analyzed metabolite ratios, mI/NAA height at TE =

35 ms gives the most accurate prediction of outcome, with 84.6% sensitivity and 95.2% specificity, within the first 96 hours of age, regardless of the postnatal age at H-MRS examination (see *Table 8 and Figure 8*).

Table 8. Results of Receiver Operating Characteristics (ROC) analysis.

mI: myo-inositol, NAA: N-acetyl-aspartate, Cr: creatine, TE: echo-time, AUC: area-under-the-ROC-curve.

Difference between ROC curves was significantly different ($p < 0.0001$) (109).

Assessed metabolite ratio	Cut-off value	AUC	Sensitivity	Specificity	Positive predictive value	Negative predictive value
mI/NAA height (TE = 35 ms)	0.6798	0.9084	84.6%	95.2%	91.7%	90.9%
mI/Cr height (TE = 35 ms)	0.6274	0.8462	61.5%	95.2%	88.9%	80.0%
NAA/Cr height (TE = 144 ms)	0.7798	0.8396	70.6%	85.3%	75.0%	75.6%

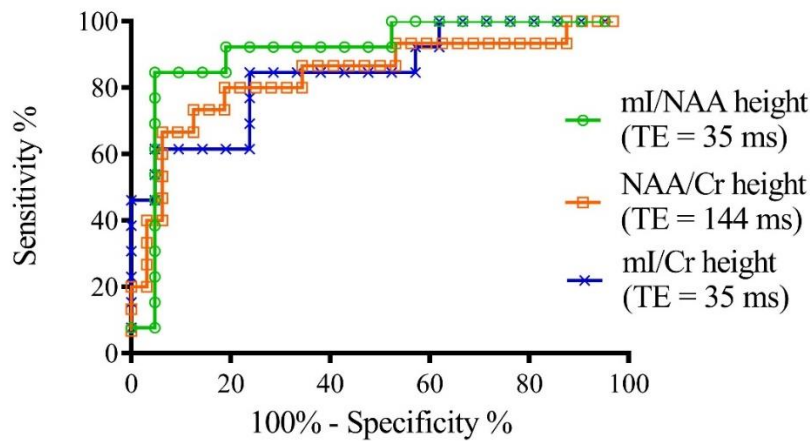


Figure 8. Receiver Operating Characteristics (ROC) curves of metabolite ratios showing no correlation with age at scan.

mI: myo-inositol, NAA: N-acetyl-aspartate, Cr: creatine, TE: echo-time.

The area under the ROC curve was 0.9084 for mI/NAA, 0.8396 for NAA/Cr and 0.8462 for mI/Cr height ($p < 0.0001$).

4.2 Optimal postnatal age at H-MRS for outcome prediction in neonatal HIE

According to the patient selection described previously, 169 infants met all the criteria and were enrolled in our 2nd study. Ninety-six of the 169 patients had the H-MRS examination performed while receiving HT, the remaining 73 patients were scanned under normothermic conditions, after the completion of HT. All newborns with early (DOL 1-3) H-MRS scans had the examination under hypothermic conditions, 6 newborns with midtime (DOL 4-6) H-MRS scan were examined during ongoing HT.

Clinical data of newborns are presented in *Table 9*, sorted according to postnatal age category at initial H-MRS examination. As seen in the table, postnatal age categories did not differ in any examined clinical parameters.

Table 9. Clinical characteristics of newborns enrolled in the study of optimal postnatal age at scan (2nd study), categorized by postnatal age at initial H-MRS.

Data shown as median [IQR], mean \pm SD or percentage. DOL: day of life, BD: base deficit.

^a moderate encephalopathy: 6 h normal amplitude-integrated electroencephalography (aEEG) pattern (continuous or discontinuous normal voltage) AND Sarnat stage 1-2, severe encephalopathy: 6h abnormal aEEG pattern (burst suppression, low voltage or flat trace) OR Sarnat stage 3 (20).

* represents significant results of χ^2 or Fisher's exact test ($p < 0.05$).

	Early H-MRS (DOL 1-3) n = 91	Midtime H-MRS (DOL 4-6) n = 50	Late H-MRS (DOL 7-14) n = 28	p value
Male sex %	63 %	37 %	61 %	0.071
Gestational age (weeks)	39 [38; 40]	40 [39; 40]	39 [37; 40]	0.298
Birth weight (g)	3175 \pm 521	3321 \pm 542	3082 \pm 528	0.126
Apgar 1'	2 [0; 3]	2 [1; 4]	2 [1; 5]	0.425
Apgar 5'	4 [3; 6]	5 [3; 6]	5 [3; 7]	0.107
Apgar 10'	5 [4; 7]	6 [5; 7]	5 [4; 7]	0.758
Onset of hypothermia (h)	1.8 [1.2; 2.5]	2.1 [1.4; 2.6]	1.8 [1.0; 2.7]	0.439
Lowest pH < 1hour of age	7.03 \pm 0.20	7.04 \pm 0.18	6.96 \pm 0.24	0.202
Highest BD < 1hour of age	17.7 \pm 6.2	16.1 \pm 6.7	16.5 \pm 7.0	0.352
Moderate/severe encephalopathy ^a	33/58	26/24	14/14	0.143

First, we analyzed the association between metabolite ratios showing highest predictive utility based on existing evidence and our previous study, as well as outcome, across all three postnatal age categories. The performed Mann-Whitney U-test revealed that only NAA/Cr height ratio, and mI/NAA height ratio and area ratio were able to discriminate between good and poor outcomes consistently throughout the early, midtime and late postnatal age windows, as well (see *Table 10* and *Figure 9*). In newborns facing good outcome, NAA/Cr height ratio was higher, and mI/NAA height and area ratios lower, compared with newborns with poor outcome, throughout all three postnatal age category. Moreover, as seen from *Table 10* and *Figure 9*, medians of metabolite ratios showed a slight shift between postnatal age categories, in the good and poor outcome groups as well.

Next, ROC analysis was performed to assess prognostic value of metabolite ratios showing association with outcome consistently through postnatal age categories, which revealed that the highest predictive value could be observed in the late (DOL 7-14) postnatal age window, represented by the highest sum of AUCs.

Detailed results of the performed ROC analysis are displayed in *Table 11*, ROC-curves are displayed in *Figure 10*.

Table 10. Results of Mann-Whitney U-test comparison of metabolite ratios and outcome, across postnatal age categories at H-MRS scan (n = 169). Data shown as median [IQR]. NAA: N-acetyl-aspartate, Cr: creatine, Cho: choline, DOL: day of life. BD: base deficit. * represents significant results (p<0.05).

	Early H-MRS (DOL 1-3)			Midtime H-MRS (DOL 4-6)			Late H-MRS (DOL ≥ 7)		
	Good n = 44	Poor n = 47	p value	Good n = 37	Poor n = 13	p value	Good n = 19	Poor n = 9	p value
NAA/Cr height	1.08 [0.97; 1.16]	0.85 [0.73; 1.02]	<0.0005*	1.09 [0.99; 1.21]	0.84 [0.52; 0.94]	<0.0005*	1.09 [0.93; 1.15]	0.69 [0.62; 0.74]	<0.0005*
NAA/Cr area	1.05 [0.94; 1.15]	0.91 [0.78; 1.02]	<0.0005*	1.00 [0.97; 1.12]	0.93 [0.67; 1.08]	0.111	0.98 [0.83; 1.12]	0.72 [0.66; 0.76]	<0.0005*
NAA/Cho height	0.95 [0.88; 1.09]	0.86 [0.74; 1.03]	0.097	0.80 [0.75; 0.92]	0.69 [0.57; 0.83]	0.167	0.65 [0.56; 0.72]	0.48 [0.42; 0.66]	0.053
NAA/Cho area	0.69 [0.62; 0.77]	0.65 [0.53; 0.75]	0.088	0.70 [0.66; 0.73]	0.55 [0.40; 0.59]	<0.0005*	0.58 [0.49; 0.65]	0.38 [0.37; 0.45]	0.001*
mI/NAA height	0.41 [0.33; 0.52]	0.57 [0.45; 0.81]	<0.0005*	0.33 [0.29; 0.44]	0.77 [0.50; 1.01]	<0.0005*	0.34 [0.24; 0.44]	0.54 [0.41; 0.89]	0.009*
mI/NAA area	0.66 [0.48; 0.91]	0.94 [0.80; 1.51]	0.004*	0.56 [0.49; 0.74]	1.02 [0.71; 1.51]	0.002*	0.49 [0.42; 0.79]	0.97 [0.53; 1.37]	0.009*

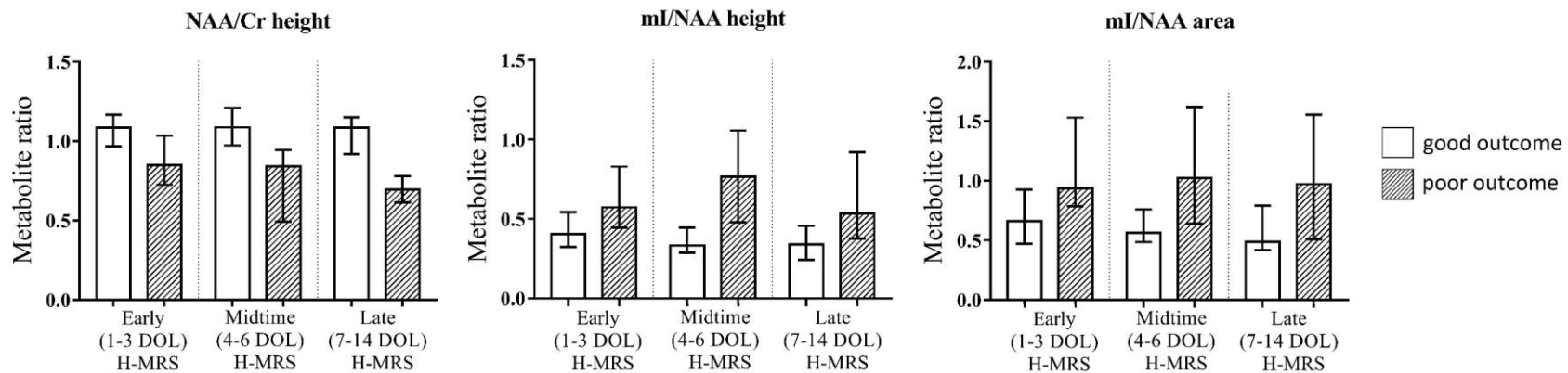


Figure 9. Metabolite ratios significantly associated with outcome throughout postnatal days 0-14, as detected in newborns with HIE facing good and poor outcome. NAA: N-acetyl-aspartate, Cr: creatine, Cho: choline, DOL: day of life. Bars represent median and interquartile range values.

Table 11. Results of Receiver-Operating Characteristics (ROC) analysis of metabolite ratios showing association with outcome throughout postnatal age categories. NAA: N-acetyl-aspartate, Cr: creatine, Cho: choline, DOL: day of life, AUC: area-under-the-ROC-curve.

	Early H-MRS (DOL 1-3)				Midtime H-MRS (DOL 4-6)				Late H-MRS (DOL 7-14)			
	AUC	cut-off	Sensitivity	Specificity	AUC	cut-off	Sensitivity	Specificity	AUC	cut-off	Sensitivity	Specificity
NAA/Cr height	0.807	0.96	81.8%	70.2%	0.871	0.95	81.1%	84.6%	0.963	0.83	88.9%	88.9%
mI/NAA height	0.719	0.42	59.0%	82.6%	0.897	0.37	63.6%	99.9%	0.816	0.42	73.7%	75.0%
mI/NAA area	0.683	0.80	69.2%	72.7%	0.818	0.85	84.8%	70.0%	0.816	0.93	99.9%	62.5%

55

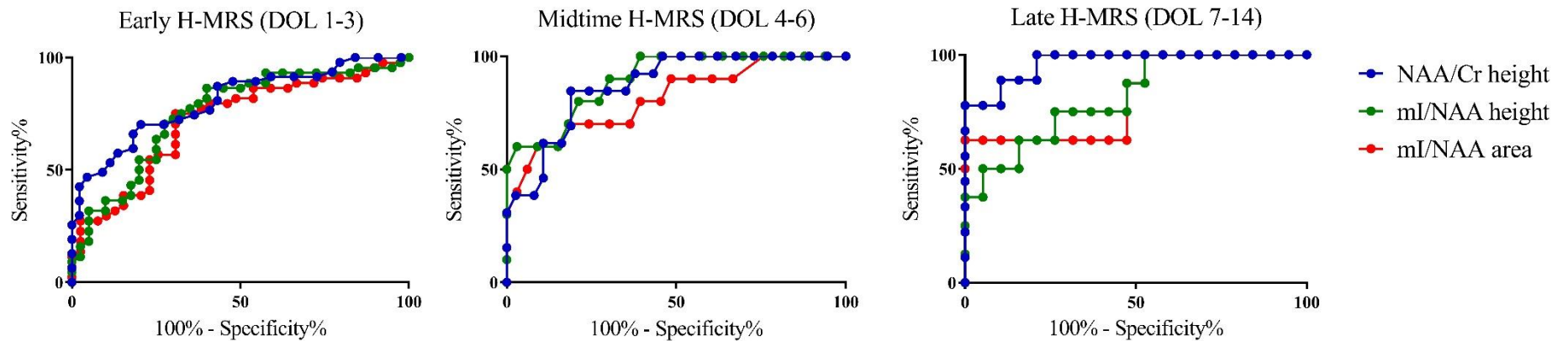


Figure 10. Receiver Operating Characteristics (ROC) curves of metabolite ratios showing association with outcome throughout postnatal age categories. NAA: N-acetyl-aspartate, Cr: creatine, Cho: choline, DOL: day of life, AUC: area-under-the-ROC-curve. AUCs are listed in *Table 11*.

4.3 Dynamic changes of H-MRS metabolite ratios in neonatal HIE

As described above, patient population for our 3rd study was identical to the one for our 2nd study, with the exception that we included not just the initial H-MRS, but all acquired H-MRS results in this analysis, without postnatal age at scan categorization. From the 169 patients enrolled, 130 neonates had only one H-MRS scan, 31 infants had only two scans, and 8 newborns had three scans, summing to a total of 216 acquired H-MRS results. Initial scans were performed on median DOL 4, second scans on median DOL 7, and third scans on median DOL 8. As detailed above, 96 of initial scans, and 12 of second scans were performed while receiving HT. All third scans were done under normothermic conditions, after the completion of HT.

Since the enrolled population is identical for the 2nd and 3rd study, clinical data of newborns are the same as presented in chapter 4.2, shown in *Table 9*.

The mixed effect model was constructed using the metabolite ratios showing consistently high predictive value throughout the first 14 days of life (i.e. all three postnatal age categories described in the 2nd study). Based on the results presented in chapter 4.2, predictive value was higher for mI/NAA height ratio than for mI/NAA area ratio, in all three postnatal age categories, therefore, we focused the mixed-effect model on NAA/Cr height ratio and mI/NAA height ratio.

Results of regression analysis are presented in *Table 12*.

Analysis of metabolite dynamics revealed that examining the whole population in general, long-term outcome was the only significant covariate for both NAA/Cr and mI/NAA height ratios ($p < 0.0001$). However, these metabolite ratios were not associated with gestational age and postnatal age.

Nevertheless, assessment of metabolite dynamics separately in the good outcome group revealed that both NAA/Cr and mI/NAA ratios were significantly affected by gestational age in newborns facing good long-term outcome ($p = 0.0058$ and 0.0002 , respectively). Furthermore, postnatal age proved to be a significant covariate for mI/NAA in this patient subgroup ($p = 0.0007$).

When analyzed separately in the poor outcome group however, the association between metabolite ratios and gestational age disappeared. Moreover, in the poor outcome group, NAA/Cr showed only slight association with postnatal age ($p = 0.0319$), whereas mI/NAA none.

Table 12. Results of mixed effect regression analysis.

Results presented separately in the whole population generally, and separately in the good and poor outcome groups.

* represents significant results ($p < 0.05$), NAA: N-acetyl-aspartate, Cr: creatine, mI: myo-inositol, w: weeks, d: days, coeff: coefficient, 95% CI: confidence interval (at 95% confidence level).

	NAA/Cr height			mI/NAA height		
	coeff	95% CI	p value	coeff	95% CI	p value
GENERAL						
(Intercept)	0.4522	(-0.3335, 1.2379)	0.2574	1.1115	(-0.2324, 2.4553)	0.1043
Gestational age (w)	0.0162	(-0.0038, 0.0362)	0.1115	-0.0177	(-0.0519, 0.0165)	0.3086
Postnatal age (d)	-0.0450	(-0.1015, 0.0114)	0.1148	-0.0467	(-0.1224, 0.0291)	0.2209
Poor outcome	-0.2277	(-0.2883, -0.1672)	<0.0001*	0.3167	(0.2125, 0.4208)	<0.0001*
GOOD OUTCOME						
(Intercept)	-0.1929	(-1.0761, 0.6902)	0.6656	1.8131	(1.1285, 2.4978)	<0.0001
Gestational age (w)	0.0320	(0.0095, 0.0545)	0.0058*	-0.0346	(-0.0521, -0.0171)	0.0002*
Postnatal age (d)	-0.0038	(-0.0723, 0.0646)	0.9088	-0.1047	(-0.1601, -0.0494)	0.0007*
POOR OUTCOME						
(Intercept)	0.7541	(-0.5712, 2.0795)	0.2600	0.5655	(-2.3818, 3.5128)	0.7025
Gestational age (w)	0.0032	(-0.0310, 0.0374)	0.8513	0.0039	(-0.0723, 0.0802)	0.9182
Postnatal age (d)	-0.0958	(-0.1824, -0.0091)	0.0319*	0.0151	(-0.1133, 0.1435)	0.8083

4.4 Prevalence and clinical presentation of CP at Semmelweis University

The query of children born between 2005 – 2015, labeled with at least one of the ICD codes listed in chapter 3.1.4, collected 1201 cases with suspected CP, after deletion of duplicates (i.e. patients labeled with more than one ICD codes and/or presented at more than one Department). Revision of these 1201 patients' medical records concluded 673 children with confirmed diagnosis of CP. From the excluded children, in 436 cases the diagnosis of CP was univocally ruled out, and in 92 cases, the information gained from the patient documentation was insufficient for clear exclusion of CP. In non-CP cases with encoded CP-related ICD-s, the most frequent alternative diagnoses were congenital hip dysplasia (5%), Down-syndrome or other genetic syndrome (5%), pes equinus (4%) and epilepsy (4%). In 23% of the excluded cases, the relevant codes were used for cranial ultrasound examination request.

Basic data, as well as data availability of these 673 patients are presented in *Table 13*.

Table 13. Basic data and data availability of patients with confirmed cerebral palsy. CP: cerebral palsy, explicitly stated: the data of interest was registered literally, word-for-word; implicitly stated: the data of interest was deduced from evaluation of patient documentation

	Number of patients, ratio (%) from all cases with confirmed CP (n = 673)
Sex (male)	394 (59%)
Clinical type of CP available	577 (86%)
• explicitly stated	445 (77%)
• implicitly stated	132 (23%)
Clinical type of CP unavailable	96 (14%)
Patient history available	602 (89%)
• negative history	98 (16%)
Patient history unavailable	71 (11%)
Mode of delivery available	391 (65%)
• vaginal birth	140 (36%)
• cesarean section	251 (64%)
Birth weight available	477 (79%)

Data availability is reported as (a) explicitly stated, constituting cases where the data of interest was registered literally, word-for-word, (b) implicitly stated, for cases where the needed information could be consistently deduced from evaluation of patient documentation, and (c) unavailable, where insufficient or no data was registered.

From cases with confirmed CP, patient history was available in 602 cases (89%). From this patient population, 330 children were born preterm (≤ 36 gestational weeks) (55%), and 108 (18%) were born with IUGR or as small for gestational age infants (SGA). PA and/or HIE was registered in the medical reports of 186 children (31%). Multiple pregnancy was noted in 112 CP cases (19%), 101 of whom (90%) were also preterm. Assisted reproductive techniques/*in vitro* fertilization (AR/IVF) was present in the history of 33 cases (5%), 24 of whom (73%) were also preterm. Infectious etiology was described in 123 cases (20%): intrauterine in 3%, perinatal in 12% and postneonatal infections in 7% of cases. Intracranial hemorrhage was registered in 161 cases (27%), while neonatal stroke in 20 cases (3%). Congenital malformation was mentioned in 74 cases (12%), while proved genetic abnormality in 16 cases (3%). It is important to note that the different etiological and risk factors were not exclusive.

From the 577 CP cases with available information concerning the clinical presentation, spastic CP was registered in 522 cases (90.5%), dyskinetic CP in 7 cases (1.2%), and ataxic CP in 3 cases (0.5%). Although the current international CP classification does not differentiate for hypotonic subtype, at the time of our study, it was noted in 45 cases (7.8%). Considering topological classification, as well, 46% of overall cases presented with spastic tetraplegia, 24% with spastic diplegia, 21% with spastic hemiplegia and 0.5% with spastic monoplegia. Severity assessed on GMFCS was definable in 82% of cases, 23% showing I grade, 24% II grade, 28% III, 20% IV grade and 9% V grade impairment.

Among the 186 cases of CP following PA (post-PA CP), 10 children had no information concerning gestational age at birth. From the 176 cases where data was available, 100 (57%) were born preterm and 76 (43%) were born at term (gestational weeks 37-42). All further descriptions are confined to these 76 children with CP born at term. Additional risk factors registered in children with post-PA CP born at term are presented in *Table 14*. Comparison of risk factor prevalence revealed that IUGR was described in

significantly more cases of post-PA CP, than in cases without PA. No other risk factor, neither distribution of prevalence ($X^2 = 12.258$, $p = 0.0565$), nor distribution of different infection subcategories ($X^2 = 4.226$, $p = 0.1209$) showed significant difference.

From these 76 post-PA cases, the clinical presentation of CP was registered in 65 cases (86%). Among these, 53 (82%) presented with spastic CP, and only 1 (1%) with ataxic CP. The historical hypotonic CP subtype was noted in 11 cases (17%). Considering localization, 55% presented with spastic tetraplegia, 14% with spastic diplegia, 11% with spastic hemiplegia and 2% with spastic monoplegia. Clinical presentation of post-PA CP are presented in *Table 15*, compared with overall clinical presentation among all cases with CP born at term, without PA. Comparison of clinical presentation showed significant difference in the prevalence of spastic tetraplegia, but in neither of the other topological categories, nor overall ($X^2 = 1.897$, $p = 0.5940$).

Table 14. Prevalence and comparison of cerebral palsy (CP) risk factors registered in children with CP born at term, following perinatal asphyxia, compared to non-asphyxiated cases.

Post-PA CP: cerebral palsy after perinatal asphyxia/hypoxic-ischemic encephalopathy, PA: perinatal asphyxia, IUGR: intrauterine growth restriction, AR/IVF: assisted reproduction/*in vitro* fertilization.

* represents significant results of Fisher's exact test ($p < 0.05$),

percentage of overall infectious cases.

Risk factor		Post-PA CP (n = 76)	CP without PA (n = 134)	p value
IUGR		7 (9%)	3 (2%)	0.038*
Infection	overall	9 (12%)	16 (12%)	>0.999
	• intrauterine	• 1 (11%) [#]	• 2 (12.5%) [#]	>0.999
	• perinatal	• 7 (78%) [#]	• 6 (37.5%) [#]	0.097
	• postneonatal	• 1 (11%) [#]	• 8 (50%) [#]	0.088
Intracranial hemorrhage		6 (8%)	13 (10%)	0.804
Neonatal stroke		1 (1%)	6 (4%)	0.426
Congenital malformation		13 (17%)	34 (25%)	0.228
Multiple pregnancy		1 (1%)	6 (4%)	0.426
AR/IVF		0 (0%)	6 (4%)	0.089

Table 15. Clinical presentation and localization registered in children with cerebral palsy (CP) born at term, following perinatal asphyxia, compared to non-asphyxiated cases.

Post-PA CP: cerebral palsy after perinatal asphyxia/hypoxic-ischemic encephalopathy, PA: perinatal asphyxia.

* represents significant results of Fisher's exact test ($p < 0.05$),

Clinical presentation		Post-PA CP (n = 65)	CP without PA (n = 127)	p value
Spastic CP	overall	53 (82%)	109 (86%)	0.529
	• tetraplegia	36 (55%)	49 (39%)	0.039*
	• diplegia	9 (14%)	27 (21%)	0.317
	• hemiplegia	7 (11%)	28 (22%)	0.102
	• monoplegia	1 (2%)	0 (0%)	0.327
Ataxic CP		1 (1%)	0 (0%)	0.339
Dyskinetic CP		0 (0%)	4 (3%)	0.302
Hypotonic CP		11 (17%)	14 (11%)	0.264

Among the 76 term post-PA cases of CP, severity of the disability was registered in 55 cases (72%), 14.5% showing grade I, 23.5% grade II, 31% grade III, 22% grade IV and 9% grade V impairment. GMFCS scores, compared among children born at term, with and without PA, are presented in *Table 16*. Comparison of severity prevalence did not show statistically significant difference neither overall, ($X^2 = 2.2739$, $p = 0.6855$), nor separately in GMFCS scale categories.

Table 16. Severity of cerebral palsy (CP) among children born at term, following perinatal asphyxia, compared to non-asphyxiated cases, registered using the Gross Motor Function Classification System (GMFCS).

Post-PA CP: following perinatal asphyxia/hypoxic-ischemic encephalopathy. PA: perinatal asphyxia.

Severity	Post-PA CP (n = 65)	CP without PA (n = 116)	p value
GMFCS I	8 (14.5%)	28 (22%)	0.080
GMFCS II	13 (23.5%)	26 (20%)	0.851
GMFCS III	17 (31%)	30 (24%)	>0.999
GMFCS IV	12 (22%)	21 (17%)	>0.999
GMFCS V	5 (9%)	11 (9%)	0.790

5 Discussion

5.1 Optimization of outcome prediction with conventional H-MRS in newborns with HIE

To the best of our knowledge, at the time of publication, our studies were the first ones that investigated the prognostic accuracy of conventional brain H-MRS performed during the first 4 postnatal days in newborns with HIE treated with HT, the effect of postnatal age on the predictive value of H-MRS throughout the first two weeks of life, as well as the combined effect of gestational age and postnatal age on metabolites.

To this end, we targeted our 1st investigation on H-MRS examinations performed the earliest possible, within 96 postnatal hours, presuming that the earlier the accurate prognostic information, the higher is its clinical importance. The predictive value of H-MRS in newborns with HIE has been widely studied, but the majority of these studies investigated H-MRS scans that were performed significantly later and/or in a wider range of postnatal age (3 to 45 postnatal days) (70,76,77,80–85,87,111), with only three papers concentrating on early neonatal ages similar to our study (54,78,79), all three analyzing considerably small patient cohorts. *Hanrahan et al* investigated newborns during their first postnatal day (31 neonates of 4-18 postnatal hours); however, considering the unstable clinical status of many severely asphyxiated infants, this may be unfeasible in the clinical practice (78). The observations of *L'Abée et al* (11 neonates of 12-48 postnatal hours) suggest that only the combined assessment of H-MRS and DWI is suitable for accurate outcome prediction (54), while *Cheong et al* (17 neonates of 48-96 postnatal hours) used absolute quantification and a custom-made head-coil to optimize data acquisition (79). Nonetheless, none of these early-acquisition studies examined newborns treated with HT. Conversely, the results of our 1st study suggest that conventional H-MRS has outstanding predictive utility as early as the first 96 postnatal hours in newborns with HIE, undergoing HT.

An additional step in our 1st study was the assessment of the association between metabolite ratios and postnatal age at scan. It has been previously described that in the early hours after hypoxic-ischemic insult, the brain undergoes extremely dynamic metabolic changes (112), so theoretically, metabolite ratios measured by H-MRS may

vary significantly depending on postnatal age at MR examination. Subsequently, the prognostic markers that vary significantly with patient age may show false negative or false positive results, if performed too early or too late in the examined time period, so would require a dynamic range of cut-off values (cut-off curve) which calls for considerably larger population and/or repeated measures. Based on these considerations, until the precise kinetics of brain metabolites are described, the proposed prognostic marker should ideally not change with postnatal age, but should only be determined by potential outcome (i.e. theoretically, severity of insult). Therefore, we focused our 1st study on metabolite ratios that were not significantly correlated with postnatal age at MR scan in the first 96 hours of life, and found that both mI/Cr, mI/NAA and NAA/Cr ratios met this criteria, hence could be potentially independent of postnatal age.

However, recent evidence suggests that the prognostic accuracy of H-MRS is not equal in the period between postnatal hours 18-96 and postnatal days 7-14 (74). Yet, the effect of the newborns' postnatal age on the predictive value of H-MRS throughout the first weeks of life has not been studied in detail, albeit examination of all newborns with HIE in a uniform postnatal narrow age window is not plausible, due to variable clinical stability and resource availability. In the 2nd research, we hypothesized that in case of metabolite ratios we found to be stable in the first 4 days of life, dynamic changes do appear in the later time periods, potentially modifying their predictive power previously observed between 5-96 hours of life. Our results suggest that whereas prognostic accuracy of these metabolite ratios slightly varies with age in the extended postnatal age windows, both NAA/Cr and mI/NAA keep their predictive power throughout the first 14 days of life, making them optimal for prediction.

This is a crucial finding, especially since current HIE guidelines recommend the performance of more than one MR examination (44), as sensitivity in prognostic prediction of various MR modalities change rapidly with the postnatal age of the newborns, as described in chapter 1.2.2.1. According to our study, it seems that certain metabolite ratios measured with H-MRS examination keep their outstanding predictive power throughout the first 14 days of life in newborns with HIE. Therefore, performing an additional H-MRS sequence whenever a brain MRI examination is done provides valuable additional diagnostic and prognostic information to the clinician.

The physiological and gestational age related variability of metabolite levels in healthy fetuses has been previously described (65). Consequently, gestational age might significantly affect absolute metabolite values and metabolite ratios in case of HIE as well, and thus modify these metabolite ratios' actual prognostic accuracy.

The results of our mixed-effect model of our 3rd study clearly show that when outcome is taken into consideration as a covariate, neither gestational age, nor postnatal age have a significant effect on NAA/Cr and mI/NAA metabolite ratios. This suggests that contrary to mild and moderate hypoxia, the severe hypoxic-ischemic injury has such a definitive impact on brain metabolism (and consequently, metabolite levels and ratios), that the influence of other modifying factors like gestational age or postnatal age disappear.

However, when these associations were analyzed in the good outcome group alone, it was revealed that these ratios are greatly influenced by gestational age, represented by a rise in NAA/Cr ratio and a decrease in mI/NAA ratio, as gestational age increases. Additionally, postnatal age turned out to be a significant covariate, but only for mI/NAA, represented by a decrease in mI/NAA with increasing postnatal age. This might imply that in case of newborns facing good outcome, the physiological, gestational age dependent variability of metabolite levels can still be observed, despite the HIE (presumably due to having undergone milder neuronal injury). Moreover, in case of mI/NAA, signs of postnatal age dependent metabolic variability also emerged.

Based on our observation, in the poor outcome group though, the effect of gestational age on metabolite ratios disappeared, suggesting that a more intense hypoxic-ischemic insult disrupts the physiological function of metabolites, and thus gestation and maturity dependent metabolite ratios. Interestingly, NAA/Cr ratio did show significant, although slight association with postnatal age, represented by decreasing NAA/Cr as postnatal age increased.

The combined results of our H-MRS studies suggest that brain H-MRS is an appropriate tool to predict neurodevelopmental outcome in newborns with HIE, at early as the first 96 postnatal hours, and consistently throughout the first 2 weeks of life, using metabolite ratios NAA/Cr and mI/NAA. Both metabolite ratios are insignificantly affected overall by both gestational age and postnatal age, which effect is greatly outweighed by these ratios' association with outcome. This emphasizes the value and utility of even

conventional H-MRS and creates the background of its widespread use in the general clinical practice, for risk stratification of newborns with HIE.

At first, it might seem surprising that none of the lactate-containing metabolite ratios included in our 1st study met the strict significance requirements of Bonferroni-correction, despite metabolite ratios such as Lac/NAA, Lac/Cr and Lac/Cho being widely studied for prognosis (54,77–79,81–84). One of the explanations for our observations is suggested by *Sijens et al*, proposing that Lac and Lac-containing metabolite ratios cease to be accurate H-MRS predictors, when analyzed in newborns treated with HT (70). This might indicate one of the working mechanisms of HT, reducing cerebral metabolic rate, glycolysis and consequential lactate production (71). Another reason for our finding might be the low quality of spectral data for Lac, when using conventional methods. In the measurements of our 1st study, SNRs of Lac peaks were extremely low, with a median [IQR] SNR of 1.0 [0.7; 1.6] without selection, and 1.6 [1.1; 2.5] after selection based on SNR = 1 criterion. However, low spectral data quality only affected peaks of Lac, since all other metabolites showed significantly more favorable signal-noise characteristics, with a median [IQR] SNR of 10.8 [8.0; 12.8] for NAA, 11.9 [8.8; 14.5] for Cho, 11.4 [7.3; 13.9] for Cr and 5.7 [4.8; 7.5] for mI, reflecting significantly better data quality. Based on these findings, we proposed that spectral peak of Lac cannot be accurately assessed and interpreted in the general clinical setting and in the absence of post-processing techniques, despite its widespread use in previous studies. Conclusively, even though we aimed our 2nd study to assess predictive value of the most frequently analyzed metabolite ratios, acquired with conventional H-MRS throughout the first 2 weeks of life, we had to exclude Lac-containing metabolites from our candidates.

Based on the above listed studies, peak area was considered to be of higher prognostic accuracy, than peak height, supported also by a meta-analysis (86). However, as detailed in chapter 1.3.3, both the assessment of peak height and peak area have their advantages and disadvantages, according to Bottomley's methodological review (89). Based on our findings, it seems that without the use of post-processing, peak height may have an appropriate predictive value and might be useful in the common clinical setting, where the use of specialized imaging and post-processing techniques is limited.

In the era of HT, the effect of cooling on brain metabolite levels is an important issue. Studies performed on rat asphyxia models suggest that HT increases the clearance of Lac upon cerebral reperfusion (113) and increases overall Lac and mI levels in the cortex, while increasing the level of taurine and decreasing the level of Cho in the thalamus (114). Moreover, *Alderliesten et al* observed that the calculated cut-off values of Lac/NAA ratio suitable for differentiation between good and poor outcome show a five-fold increase when determined under hypothermic conditions, compared to normothermia (84). Nevertheless, these findings do not conclude that thalamic mI/NAA values are also affected by cooling. Further studies would be needed to describe the hypothermia-induced changes in metabolites detected by H-MRS. However, the design of these studies raises serious methodological and ethical questions, as withdrawal of HT for moderate-to-severe HIE babies in order to establish the control group would be unethical.

5.1.1 Limitations

Despite our careful preparation of our study methodologies, there are limitations that should be taken into consideration.

First, all our H-MRS studies are retrospective in nature, therefore we could not control for factors possibly affecting the findings such as the imaging process and the clinical parameters. On the one hand, this is a limitation compared to a prospective study with fine-tuned imaging and clinical parameters for research purposes; on the other hand, this could be viewed as a strength from a clinical point of view, having relied on data obtainable from any MR facility dealing with neonatal HIE, thus being more generalizable.

Second, the difference between the sizes of the outcome groups in all three H-MRS studies is a limitation, as it underpowers our analysis. Moreover, some may criticize our approach, and may state that all neonates should be examined at the exact same age, which would enable prognostic results to be as accurate as possible. However, considering that infants cannot be assessed before reaching certain clinical stability, this would not be a realistic expectation in the overall clinical practice.

Furthermore, the general limitation of our 2nd study is the lack of healthy, gestational age specific reference data from the first two weeks of the neonatal period. However, this

would be an unrealistic anticipation – from both ethical and methodological reasons –, and theoretically, the missing referential data is not vital for prognosis.

Additionally, the establishment of postnatal age categories by itself, for analysis of prognostic performance of HMRS in our 2nd study, can be considered a limitation, since it inevitably creates artificial conditions. While assessment of postnatal age at scan in considerably smaller age categories (i.e. 6 or 12 hour periods), or as a continuous variable would be less artificial and more accurate approach to determine predictive value during the examined postnatal period, that would require such a large sample size that might only be feasible in a future multicenter study.

Finally, due to resource availability, two different 3 Tesla MRI scanners were used to examine our patient population. While this might bias the acquired spectral data, the identical magnetic field strength of the scanners, as well as our assessment of metabolite ratios instead of absolute metabolite levels counteracts this technical issue.

Clearly, our observations strongly support the value of a such future study in a larger population and on other vendors' MR scanner, in order to refine and optimize the prognostic power of H-MRS.

5.2 Prevalence and clinical presentation of CP at Semmelweis University

To our knowledge, our analysis is the first to assess the prevalence, etiological and clinical classification of CP in the Central Hungary region. Previously, similar published study was conducted in Borsod-Abaúj-Zemplén county, analyzing frequencies in children with CP born between 1994-2006 (98). Moreover, another research from Southwest Hungary (counties Baranya, Somogy and Tolna) analyzed the usefulness of an MRI classification system in determining the etiology of CP, in a cohort of children with CP born between 1990-2015 (115).

Comparison of these three studies conclude that prevalence of both prematurity (55% vs 31% vs 36%), both PA (31% vs 19% vs 10%) was higher in the Semmelweis cohort, than in the cohorts from Borsod-Abaúj-Zemplén county and Southwestern Hungary, respectively. The explanation could be that while the later studies analyzed representative regional data, our research investigated center data, including more severe neonates,

considering our university's role as a center for extremely preterm infants and for HIE. However, SGA was registered less frequently in our analysis compared with data from Borsod-Abaúj-Zemplén county (18% vs 30%), presumably due to lower incidence of SGA births in Central Hungary compared with Borsod-Abaúj-Zemplén county (4.5% vs 12%, based on the data of Hungarian Central Statistical Office for year 2005). Nevertheless, the differences in prevalence could be related to the different methodology and examined period (2005-2015 vs 1994-2006). Clinical classification based on physiology (muscle tone abnormality) cannot be compared due to data unavailability concerning CP cases in Borsod-Abaúj-Zemplén and Southwestern Hungary. On the other hand, topological classification was similar in our cohort than in Borsod-Abaúj-Zemplén county in terms of unilateral palsy (20% vs 19%), but differed in terms of bilateral palsy (68% vs 60%), probably due to the highly increased incidence of HIE at our university.

Compared with international registry data, the prevalence of both prematurity (55% vs 35%), both HIE (31% vs 2-10%) was revealed in more children with CP in our study. Intracranial hemorrhage and neonatal stroke accounted for 17% of CP cases according to a Swedish study, greatly exceeded by our respective data of 30% (7). These findings could also be explained with the high progressivity level of our university's NICUs, as well as intensive follow-up of affected children. As for infectious etiology, intrauterine infections were described in 5% of CP international cases, comparable to our data of 3% (100). Neonatal central nervous system infections are seen in 3% of cases based on the above mentioned Swedish research, whereas we registered them in 12% of cases (7). Congenital malformations are registered in 11-32% of cases based on international studies – similar to our observation of 12% –, whereas malformations of the central nervous system appear in 12% of CP cases based on international registries, compared to 5% registered by our study (116). Clinical classification based on physiology shows that internationally, spastic subtype is determined in 72-91% of cases (102), dyskinetic CP in 15% (103), and ataxic subtype in 4-5% (104), whereas we registered these subtypes in 90.5%, 1.2% and 0.5% of cases, respectively. As for topological classification, international registries recorded hemiplegia in 21-36%, diplegia in 13-45%, tetraplegia in 9-44% of all CP cases, compared to our relevant incidences being 23% for hemiplegia, 24% for diplegia and 46% for tetraplegia. This shows similar frequencies of CP subtypes, except a slightly increased incidence of spastic tetraplegia, presumably due to the exceptionally high prevalence of

prematurity and HIE in our patient population, as discussed previously. These differences might also be related to the methodological dissimilarities between registries, underscoring the need for data collection guidelines and the establishment of a national CP registry, conform international recommendations (102).

While it is well-established that the principle CP manifestation for children with previous HIE is bilateral spastic CP (especially tetraplegia) and dyskinetic CP – reported having a combined frequency of 94% (117) –, however, the precise incidence of the different CP subtypes is not often detailed in outcome studies. One small study reported CP subtype incidences being 85% spastic CP – that could be divided to 70% spastic tetraplegia and 15% hemiplegia – as well as 15% dyskinetic CP (92). Another analysis detected that 67% of children with HIE had spastic CP – 56% tetraplegia and 11% hemiplegia – additional to 33% having dyskinetic CP (118). Surprisingly, our observations only partly comply with these concordant results, reporting spastic CP in 82% of cases – divided as 55% tetraplegia, 14% diplegia and 11% hemiplegia –; as well as no cases of dyskinetic CP. We believe that the increased incidence of diplegia could be a methodological issue, considering that diplegia and tetraplegia only differ in the upper limb involvement (which show only fine motor impairment in diplegia, but more severe palsy in tetraplegia). In our study, we observed surprisingly low incidence of dyskinetic CP compared with international data (0% vs 15-33% following HIE, and 1% vs 15% overall). This phenomenon needs further analysis. Conversely, the historical subtype of hypotonic CP was recorded in 17% of cases with HIE, despite it having been excluded from the CP categorization system by SCPE (102). This again emphasized the need for standardization of patient documentation in the national CP management, crucial for a future CP registry with uniform eligibility criteria.

5.2.1 Limitations

The most important methodological issue of our study is the query based on ICD codes. This can be highly distorted by the financial aspect of their uses, presumably sometimes coding commonly used ICD codes, as opposed to the ones accurately describing the CP subtype. However, since our analysis was an audit focused study to assess feasibility, our results imply the need for quality management concerning patient documentation, to acquire more precise incidence data in the future.

In terms of comparison with other studies describing CP prevalence, the difference in patient selection and examined time period could be a significant confounding factor, since the prevalence of the different subtypes as well as severity depends on the incidence of different risk factors in the examined region/hospital, and also of the standard management of children with CP in the area of interest.

Due to the examined time period in our study (2005-2015), the historical subtype of hypotonic CP was registered in a considerable number of cases – who would otherwise increase the size of another subtype cohort – possibly distorting our incidence data.

Nevertheless, overall, CP prevalence do comply with international data, and the observed differences are an important feedback. Thus, the conclusions of our study considering documentation and standardization prerequisites constitute an important founding stone for a future Hungarian CP registry.

6 Conclusion

1. Conventional brain proton MR spectroscopy is a useful tool in predicting neurological outcome as early as the first 96 postnatal hours in newborns with hypoxic-ischemic encephalopathy, analyzing metabolite ratio myo-inositol/N-acetyl-aspartate, with 84.6% sensitivity, 95.2% specificity and no correlation with postnatal age.
2. Conventional brain proton MR spectroscopy and namely, metabolite ratios N-acetyl-aspartate/creatine and myo-inositol/N-acetyl-aspartate have an outstanding predictive value throughout the first 14 days of life in asphyxiated newborns, with the highest predictive accuracy after postnatal day 6.
3. Metabolite ratios N-acetyl-aspartate/creatine and myo-inositol/N-acetyl-aspartate are associated with gestational age during the first 2 weeks of life in asphyxiated newborns facing good outcome, suggesting that physiological maturation determined variations of brain metabolism are not abolished in these cases; however, these variations disappear in newborns facing poor outcome, suggesting that such severe insult disrupts physiological cerebral processes.
4. N-acetyl-aspartate/creatine ratio was affected by postnatal age in the first 2 weeks of life of asphyxiated newborns potentially having good outcome, whilst myo-inositol/N-acetyl-aspartate was associated with postnatal age in infants facing poor outcome.
5. Insult severity and consequential outcome in neonatal hypoxic-ischemic encephalopathy has such a high impact on metabolite levels measured by conventional brain proton MR spectroscopy that it outweighs the effect of gestational age and postnatal age on metabolite ratios, making brain proton MR spectroscopy a reliable prognostic tool in moderate-to-severe neonatal hypoxic-ischemic encephalopathy.
6. In a large pediatric cohort of Central Hungary born between 2005-2015, the incidence of perinatal asphyxia/hypoxic-ischemic encephalopathy in the history of children diagnosed with cerebral palsy is 31% (35% in term infants), divided based on physiology to 82% spastic subtype, divided based on topology to 55% spastic tetraplegia, 14% spastic diplegia and 11% spastic hemiplegia, as well as 1% ataxic subtype and 0% dyskinetic subtype (with the historical category of hypotonic form seen in 17%).

7 Summary

Early and accurate prediction of neurodevelopmental outcome in newborns with moderate-to-severe hypoxic-ischemic encephalopathy (HIE) has increasing importance, in order to select newborns who would benefit the most from future compound neuroprotective strategies. Thus, we aimed to optimize outcome prediction with conventional brain proton MR spectroscopy (H-MRS), on newborns treated with HIE at the Neonatal Intensive Care Unit, of the 1st Department of Pediatrics, Semmelweis University. Moreover, as cerebral palsy (CP) constitutes the most severe adverse outcome in survivors, we assessed the prevalence of HIE as a risk factor among children diagnosed with CP at the clinics of Semmelweis University, as well as the observed clinical presentation and severity.

First, we established that conventionally acquired proton MR spectroscopy H-MRS is suitable for outcome prediction, as early as the first 4 postnatal days HIE neonates, with highest predictive value for myo-inositol (mI)/N-acetyl-aspartate (NAA), showing sensitivity of 84.6% and specificity of 95.2%, and moreover, presenting weak correlation with postnatal age at scan in this time period. Second, we recognized that conventional H-MRS keeps its predictive value throughout postnatal days 0-14, for metabolite ratios NAA/creatinine (Cr) and mI/NAA, with the highest predictive accuracy between postnatal days 7-14. Third, we discovered that neither gestational age, nor postnatal age significantly affected these metabolite ratios in the first 2 weeks of life, and they showed strongest association with outcome. Additionally, we observed that gestational age dependent variations of these metabolite ratios do appear in newborns facing good outcome, however, this association disappears in the poor outcome group. This is presumably due to disrupted physiological maturation associated metabolic processes in case of adverse outcome. Finally, we described that the incidence of perinatal asphyxia (PA) as a risk factor was 31% among children diagnosed with CP in a representative Hungarian cohort between 2005-2015. The most frequently observed CP subtype based on muscle tone was spastic subtype, seen in 82% of former PA cases suffering from CP, divided as 55% tetraplegia, 14% diplegia and 11% hemiplegia in these children.

We conclude that H-MRS is a valuable, generalizable and gestational age independent tool for risk stratification of newborns with HIE, as early as the first 4 days, and throughout the first 2 postnatal weeks, irrespective of postnatal age at scan.

8 Összefoglalás

A közepsúlyos-súlyos hypoxiás-ischemiás encephalopathiával (HIE) érintett újszülöttek fejlődésneurológiai kimenetelének korai és pontos előrejelzése kiemelkedő fontosságú a jövőbeli neuroprotektív stratégiák bevezetésével leginkább profitáló csecsemők kiválasztására. Célkitűzésünk éppen ezért a konvencionális agyi proton MR spektroszkópia (H-MRS) prediktív értékének optimalizációja volt, a Semmelweis Egyetem 1. sz. Gyermekgyógyászati Klinika Perinatális Intenzív Centrumán HIE-vel kezelt újszülöttek körében. Mivel a túlélők legsúlyosabb szövődménye a cerebrális parézis (CP), felmértük a HIE rizikófaktor előfordulását a Semmelweis Egyetem klinikáin CP-vel kezelt gyerekek körében, valamint a klinikai formát és súlyosságot.

Megállapítottuk elsőként, hogy a konvencionális H-MRS már a HIE-vel érintett újszülöttek első 4 életnapja során alkalmas a kimenetel előrejelzésére, a legmagasabb prediktív értéket pedig a mio-inozitol (mI)/N-acetil-aszpartát arány mutatta, 84,6% szenzitivitással és 95,2% specificitással, emellett ez a metabolit arány gyenge korrelációt mutatott az életkorral a vizsgált időablakban. Ezt követően igazoltuk, hogy a konvencionális H-MRS megtartja prediktív értékét a 0-14. életnapokon keresztül, az NAA/kreatin (Cr) és a mI/NAA arányok esetén. A legpontosabb előrejelzést a 7-14. életnapok közt mértük. Harmadik vizsgálatunkban leírtuk, hogy sem a gesztációs kor, sem pedig az életkor nem befolyásolja szignifikánsan ezen metabolit arányokat az első 2 élethét során, melyek csupán a kimenetellel mutatnak erős összefüggést. Megfigyeltük továbbá, hogy bár a gesztációs korról összefüggő metabolit változások megjelennek a jó kimenetelű újszülöttekben, ezek az összefüggések eltűnnek a rossz kimenetelű csoportban. Feltételezzük, hogy ez a súlyos kimenetel esetén megszakadó, fiziológias érissel összefüggő anyagcsere-folyamatokkal magyarázható. Végül leírtuk, hogy a perinatalis asphyxia (PA) rizikófaktor előfordulása 31% a CP-s gyerekek körében, egy reprezentatív magyarországi minta alapján 2005-2015 között. A leggyakoribb CP altípus a spasztikus forma, melyet a PA-t követően kialakult CP 82%-ában írtak le, míg topológia szerint tetraplégia 55%-ban, diplégia 14%-ban, hemiplégia pedig 11%-ban került leírásra.

Következtetésünk alapján a H-MRS értékes, általánosan használható, és gesztációs kortól független eszköz a HIE-vel érintett újszülöttek kimenetelének előrejelzésére, már az első 4 életnap során és folyamatosan az első 2 élethétén át, függetlenül a vizsgálat időpontjától.

9 Bibliography

1. Kurinczuk JJ, White-Koning M, Badawi N. (2010) Epidemiology of neonatal encephalopathy and hypoxic-ischaemic encephalopathy. *Early Hum Dev*, 86: 329–338.
2. Liu L, Johnson HL, Cousens S, Perin J, Scott S, Lawn JE, Rudan I, Campbell H, Cibulskis R, Li M, Mathers C, Black RE, Child Health Epidemiology Reference Group of WHO and UNICEF. (2012) Global, regional, and national causes of child mortality: an updated systematic analysis for 2010 with time trends since 2000. *Lancet*, 379: 2151–2161.
3. Kelen D, Robertson NJ. (2010) Experimental treatments for hypoxic ischaemic encephalopathy. *Early Hum Dev*, 86: 369–377.
4. Volpe JJ. Hypoxic-Ischemic Encephalopathy. In: *Neurology of the Newborn*, 5th Edition. Elsevier, Amsterdam, 2008: 247–282.
5. Badawi N, Kurinczuk JJ, Keogh JM, Alessandri LM, O’Sullivan F, Burton PR, Pemberton PJ, Stanley FJ. (1998) Intrapartum risk factors for newborn encephalopathy: the Western Australian case-control study. *BMJ*, 317: 1554–1558.
6. Herlenius E, Kuhn P. (2013) Sudden unexpected postnatal collapse of newborn infants: a review of cases, definitions, risks, and preventive measures. *Transl Stroke Res*, 4: 236–247.
7. Hagberg B, Hagberg G, Beckung E, Uvebrant P. (2001) Changing panorama of cerebral palsy in Sweden. VIII. Prevalence and origin in the birth year period 1991–94. *Acta Paediatr*, 90: 271–277.
8. McIntyre S, Badawi N, Blair E, Nelson KB. (2015) Does aetiology of neonatal encephalopathy and hypoxic-ischaemic encephalopathy influence the outcome of treatment? *Dev Med Child Neurol*, 57: 2–7.
9. Cowan F, Rutherford M, Groenendaal F, Eken P, Mercuri E, Bydder GM, Meiners LC, Dubowitz LMS, de Vries LS. (2003) Origin and timing of brain lesions in term infants with neonatal encephalopathy. *Lancet*, 361: 736–742.
10. Badawi N, Kurinczuk JJ, Keogh JM, Alessandri LM, O’Sullivan F, Burton PR, Pemberton PJ, Stanley FJ. (1998) Antepartum risk factors for newborn encephalopathy: the Western Australian case-control study. *BMJ*, 31: 1549–1553.
11. Holowach-Thurston J, Hauhart RE, Jones EM, Ikossi MG, Pierce RW. (1973) Decrease in brain glucose in anoxia in spite of elevated plasma glucose levels. *Pediatr Res*, 7: 691–695.
12. Lorek A, Takei Y, Cady EB, Wyatt JS, Penrice J, Edwards AD, Peebles D, Wylezinska M, Owen-Reece H, Kirkbride V. (1994) Delayed (“secondary”) cerebral energy failure after acute hypoxia-ischemia in the newborn piglet:

- continuous 48-hour studies by phosphorus magnetic resonance spectroscopy. *Pediatr Res*, 36: 699–706.
13. Kusaka T, Matsuura S, Fujikawa Y, Okubo K, Kawada K, Namba M, Okada H, Imai T, Isobe K, Itoh S. (2004) Relationship between cerebral interstitial levels of amino acids and phosphorylation potential during secondary energy failure in hypoxic-ischemic newborn piglets. *Pediatr Res*, 55: 273–279.
 14. Barks JD, Silverstein FS. (1992) Excitatory amino acids contribute to the pathogenesis of perinatal hypoxic-ischemic brain injury. *Brain Pathol*, 2: 235–243.
 15. Gilland E, Puka-Sundvall M, Hillered L, Hagberg H. (1998) Mitochondrial function and energy metabolism after hypoxia-ischemia in the immature rat brain: involvement of NMDA-receptors. *J Cereb Blood Flow Metab Off J Int Soc Cereb Blood Flow Metab*, 18: 297–304.
 16. Wyatt JS, Edwards AD, Azzopardi D, Reynolds EO. (1989) Magnetic resonance and near infrared spectroscopy for investigation of perinatal hypoxic-ischaemic brain injury. *Arch Dis Child*, 64: 953–963.
 17. Fleiss B, Gressens P. Tertiary mechanisms of brain damage: a new hope for treatment of cerebral palsy? (2012) *Lancet Neurol*, 11: 556–566.
 18. Hassell KJ, Ezzati M, Alonso-Alconada D, Hausenloy DJ, Robertson NJ. (2015) New horizons for newborn brain protection: enhancing endogenous neuroprotection. *Arch Dis Child Fetal Neonatal Ed*, 100: F541–552.
 19. Sarnat HB, Sarnat MS. (1976) Neonatal encephalopathy following fetal distress. A clinical and electroencephalographic study. *Arch Neurol*, 33: 696–705.
 20. Shalak LF, Laptook AR, Velaphi SC, Perlman JM. (2003) Amplitude-integrated electroencephalography coupled with an early neurologic examination enhances prediction of term infants at risk for persistent encephalopathy. *Pediatrics*, 111: 351–357.
 21. Thompson CM, Puterman AS, Linley LL, Hann FM, van der Elst CW, Molteni CD, Malan AF. (1997) The value of a scoring system for hypoxic ischaemic encephalopathy in predicting neurodevelopmental outcome. *Acta Paediatr*, 86: 757–761.
 22. Merchant N, Azzopardi D. (2015) Early predictors of outcome in infants treated with hypothermia for hypoxic-ischaemic encephalopathy. *Dev Med Child Neurol*, 57: 8–16.
 23. de Vries LS, Toet MC. (2006) Amplitude integrated electroencephalography in the full-term newborn. *Clin Perinatol*, 33: 619–632.
 24. Csekő A, Bangó M, Lakatos P, Kárdási J, Pusztai L, Szabó M. (2013) Accuracy of amplitude-integrated electroencephalography in the prediction of

- neurodevelopmental outcome in asphyxiated infants receiving hypothermia treatment. *Acta Paediatr*, 102: 707–711.
25. Kovács K, Szakmár E, Méder Ü, Kolossváry M, Bagyura Z, Lamboy L, Élő Zs, Szabó A, Szabó M, Jermendy Á. (2017) [Hypothermia treatment in asphyxiated neonates – a single center experience in Hungary]. *Orv Hetil*, 158: 331–339.
 26. Perlman JM, Tack ED, Martin T, Shackelford G, Amon E. (1989) Acute systemic organ injury in term infants after asphyxia. *Am J Dis Child*, 143: 617–620.
 27. The TOBY Study Group, Azzopardi D, Brocklehurst P, Edwards D, Halliday H, Levene M, Thoresen M, Whitelaw A. (2008) The TOBY Study. Whole body hypothermia for the treatment of perinatal asphyxial encephalopathy: A randomised controlled trial. *BMC Pediatr*, 8: 17.
 28. Azzopardi DV, Edwards AD, Halliday HL, Kapellou O, Porter E, Whitelaw A. (2009) Moderate hypothermia to treat perinatal asphyxial encephalopathy. *N Engl J Med*, 361: 1349-1358.
 29. Gunn AJ, Bennet L, Gunning MI, Gluckman PD, Gunn TR. (1999) Cerebral hypothermia is not neuroprotective when started after postischemic seizures in fetal sheep. *Pediatr Res*, 46: 274–280.
 30. Polderman KH, Herold I. (2009) Therapeutic hypothermia and controlled normothermia in the intensive care unit: practical considerations, side effects, and cooling methods. *Crit Care Med*, 37: 1101–1120.
 31. Favié LMA, Groenendaal F, van den Broek MPH, Rademaker CMA, de Haan TR, van Straaten HLM, Dijk PH, van Heijst A, Dudink J, Dijkman KP, Rijken M, Zonnenberg IA, Cools F, Zecic A, van der Lee JH, Nuytemans DH, van Bel F, Egberts TCG, Huitema ADR. (2019) Pharmacokinetics of morphine in encephalopathic neonates treated with therapeutic hypothermia. *PLoS One*, 14: e0211910.
 32. Laptook AR, Corbett RJ, Sterett R, Garcia D, Tollefsbol G. (1995) Quantitative relationship between brain temperature and energy utilization rate measured in vivo using ³¹P and ¹H magnetic resonance spectroscopy. *Pediatr Res*, 38: 919–925.
 33. Gunn AJ, Thoresen M. (2006) Hypothermic neuroprotection. *NeuroRx*, 3: 154-169.
 34. Edwards AD, Brocklehurst P, Gunn AJ, Halliday H, Juszczak E, Levene M, Strohm B, Thoresen M, Whitelaw A, Azzopardi D. (2010) Neurological outcomes at 18 months of age after moderate hypothermia for perinatal hypoxic ischaemic encephalopathy: synthesis and meta-analysis of trial data. *BMJ*, 340: c363.
 35. Ahmad QM, Chishti AL, Waseem N. (2018) Role of melatonin in management of hypoxic ischaemic encephalopathy in newborns: A randomized control trial. *J Pak Med Assoc*, 68: 1233–1237.

36. Aly H, Elmahdy H, El-Dib M, Rowisha M, Awany M, El-Gohary T, Elbatch M, Hamisa M, El-Mashad AR. (2015) Melatonin use for neuroprotection in perinatal asphyxia: a randomized controlled pilot study. *J Perinatol*, 35: 186–191.
37. Marti HH, Bernaudin M, Petit E, Bauer C. (2000) Neuroprotection and angiogenesis: dual role of erythropoietin in brain ischemia. *News Physiol Sci*, 15: 225–229.
38. Oorschot DE, Sizemore RJ, Amer AR. (2020) Treatment of neonatal hypoxic-ischemic encephalopathy with erythropoietin alone, and erythropoietin combined with hypothermia: history, current status, and future research. *Int J Mol Sci*, 21: 1487.
39. Ren C, Gao X, Niu G, Yan Z, Chen X, Zhao H. (2008) Delayed postconditioning protects against focal ischemic brain injury in rats. *PLoS One*, 3: e3851.
40. Pignataro G, Esposito E, Sirabella R, Vinciguerra A, Cuomo O, Di Renzo G, Annunziato L. (2013) nNOS and p-ERK involvement in the neuroprotection exerted by remote postconditioning in rats subjected to transient middle cerebral artery occlusion. *Neurobiol Dis*, 54: 105–114.
41. Ezzati M, Bainbridge A, Broad KD, Kawano G, Oliver-Taylor A, Rocha-Ferreira E, Alonso-Alconada D, Fierens I, Rostami J, Jane Hassell K, Tachtsidis I, Gressens P, Hristova M, Bennett K, Lebon S, Fleiss B, Yellon D, Hausenloy DJ, Golay X, Robertson NJ. (2016) Immediate remote ischemic postconditioning after hypoxia ischemia in piglets protects cerebral white matter but not grey matter. *J Cereb Blood Flow Metab*, 36: 1396–1411.
42. Dixon B, Reis C, Ho W, Tang J, Zhang J. (2015) Neuroprotective strategies after neonatal hypoxic ischemic encephalopathy. *Int J Mol Sci*, 16: 22368–22401.
43. Thoresen M, Tooley J, Liu X, Jary S, Fleming P, Luyt K, Jain A, Cairns P, Harding D, Sabir H. (2013) Time is brain: starting therapeutic hypothermia within three hours after birth improves motor outcome in asphyxiated newborns. *Neonatology*, 104: 228–233.
44. American College of Obstetricians and Gynecologists (2014) Executive summary: Neonatal encephalopathy and neurologic outcome, second edition. Report of the American College of Obstetricians and Gynecologists' Task Force on Neonatal Encephalopathy. *Obstet Gynecol*, 123: 896–901.
45. Reynolds PR, Dale RC, Cowan FM. (2001) Neonatal cranial ultrasound interpretation: a clinical audit. *Arch Dis Child Fetal Neonatal Ed*, 84: F92-95.
46. Ment LR, Bada HS, Barnes P, Grant PE, Hirtz D, Papile LA, Pinto-Martin J, Rivkin M, Slovis TL. (2002) Practice parameter: neuroimaging of the neonate: report of the Quality Standards Subcommittee of the American Academy of Neurology and the Practice Committee of the Child Neurology Society. *Neurology*, 58: 1726–1738.

47. Wezel-Meijler G, de Vries LS. (2014) Cranial Ultrasound - Optimizing Utility in the NICU. *Curr Pediatr Rev*, 10: 16–27.
48. Counsell SJ, Rutherford MA. (2002) Magnetic resonance imaging of the newborn brain. *Curr Paediatr*, 12: 401–413.
49. Schild HH. MRI made easy, 2nd edition. S.l. Schering, Berlin, 1997: 7-100.
50. Barkovich AJ, Westmark K, Partridge C, Sola A, Ferriero DM. (1995) Perinatal asphyxia: MR findings in the first 10 days. *AJNR Am J Neuroradiol*, 16: 427–438.
51. Rutherford MA, Pennock JM, Counsell SJ, Mercuri E, Cowan FM, Dubowitz LM, Edwards AD. (1998) Abnormal magnetic resonance signal in the internal capsule predicts poor neurodevelopmental outcome in infants with hypoxic-ischemic encephalopathy. *Pediatrics*, 102: 323–328.
52. Thakur NH, Spencer AJ, Kilbride HW, Lowe LH. (2013) Findings and patterns on MRI and MR spectroscopy in neonates after therapeutic hypothermia for hypoxic ischemic encephalopathy treatment. *South Med J*, 106: 350–355.
53. Cowan FM, Pennock JM, Hanrahan JD, Manji KP, Edwards AD. (1994) Early detection of cerebral infarction and hypoxic ischemic encephalopathy in neonates using diffusion-weighted magnetic resonance imaging. *Neuropediatrics*, 25: 172–175.
54. L’Abee C, de Vries LS, van der Grond J, Groenendaal F. (2005) Early Diffusion-Weighted MRI and 1H-Magnetic Resonance Spectroscopy in Asphyxiated Full-Term Neonates. *Neonatology*, 88: 306–312.
55. Alderliesten T, de Vries LS, Benders MJNL, Koopman C, Groenendaal F. (2011) MR Imaging and Outcome of Term Neonates with Perinatal Asphyxia: Value of Diffusion-weighted MR Imaging and H MR Spectroscopy. *Radiology*, 261: 235–242.
56. Massaro AN, Evangelou I, Fatemi A, Vezina G, Mccarter R, Glass P, Limperopoulos C. (2015) White matter tract integrity and developmental outcome in newborn infants with hypoxic-ischemic encephalopathy treated with hypothermia. *Dev Med Child Neurol*, 57: 441–448.
57. Groenendaal F, De Vries LS. (2017) Fifty years of brain imaging in neonatal encephalopathy following perinatal asphyxia. *Pediatr Res*, 81: 150-155.
58. Tognarelli JM, Dawood M, Shariff MIF, Grover VPB, Crossey MME, Cox IJ, Taylor-Robinson S, McPhail MJW. (2015) Magnetic Resonance Spectroscopy: Principles and Techniques: Lessons for Clinicians. *J Clin Exp Hepatol*, 5: 320–328.
59. Blüml S. Magnetic Resonance Spectroscopy: Basics. In: Blüml S, Panigrahy A, (ed.) *MR Spectroscopy of Pediatric Brain Disorders*. Springer, New York, 2013: 11–23.

60. Panigrahy A, Nelson MD, Blüml S. (2010) Magnetic resonance spectroscopy in pediatric neuroradiology: clinical and research applications. *Pediatr Radiol*, 40: 3-30.
61. Scarabino T, Popolizio T, Bertolino A, Salvolini U. (1999) Proton magnetic resonance spectroscopy of the brain in pediatric patients. *Eur J Radiol*, 30: 142–153.
62. Moffett J, Ross B, Arun P, Madhavarao C, Namboodiri A. (2007) N-Acetylaspartate in the CNS: From neurodiagnostics to neurobiology. *Prog Neurobiol*, 81: 89–131.
63. Baslow MH. (2002) Evidence supporting a role for N-acetyl-L-aspartate as a molecular water pump in myelinated neurons in the central nervous system. An analytical review. *Neurochem Int*, 40: 295–300.
64. Chakraborty G, Mekala P, Yahya D, Wu G, Ledeen RW. (2001) Intraneuronal N-acetylaspartate supplies acetyl groups for myelin lipid synthesis: evidence for myelin-associated aspartoacylase. *J Neurochem*, 78: 736–745.
65. Dezortova M, Hajek M. (2008) 1H MR spectroscopy in pediatrics. *Eur J Radiol*, 67: 240–249.
66. Robertson NJ, Thayyil S, Cady EB, Raivich G. (2014) Magnetic Resonance Spectroscopy Biomarkers in Term Perinatal Asphyxial Encephalopathy: From Neuropathological Correlates to Future Clinical Applications. *Curr Pediatr Rev*, 10: 37–47.
67. Joncquel-Chevalier Curt M, Voicu PM, Fontaine M, Dessein AF, Porchet N, Mention-Mulliez K, Dobbelaere D, Soto-Ares G, Cheillan D, Vamecq J. (2015) Creatine biosynthesis and transport in health and disease. *Biochimie*, 119: 146–165.
68. Brighina E, Bresolin N, Pardi G, Rango M. (2009) Human Fetal Brain Chemistry as Detected by Proton Magnetic Resonance Spectroscopy. *Pediatr Neurol*, 40: 327–342.
69. Macrì MA, D'Alessandro N, Di Giulio C, Di Iorio P, Di Luzio S, Giuliani P, Bianchi G, Esposito E. (2005) Regional changes in the metabolite profile after long-term hypoxia-ischemia in brains of young and aged rats: a quantitative proton MRS study. *Neurobiol Aging*, 27: 98–104.
70. Sijens PE, Wischniowsky K, Ter Horst HJ. (2017) The prognostic value of proton magnetic resonance spectroscopy in term newborns treated with therapeutic hypothermia following asphyxia. *Magn Reson Imaging*, 42: 82–87.
71. Erecinska M, Thoresen M, Silver IA. (2003) Effects of hypothermia on energy metabolism in Mammalian central nervous system. *J Cereb Blood Flow Metab*, 23: 513–530.

72. Robertson NJ, Cox IJ, Cowan FM, Counsell SJ, Azzopardi D, Edwards AD. (1999) Cerebral Intracellular Lactic Alkalosis Persisting Months after Neonatal Encephalopathy Measured by Magnetic Resonance Spectroscopy. *Pediatr Res*, 46: 287–296.
73. Graham SH, Meyerhoff DJ, Bayne L, Sharp FR, Weiner MW. (1994) Magnetic resonance spectroscopy of N-acetylaspartate in hypoxic–ischemic encephalopathy. *Ann Neurol*, 35: 490–494.
74. Shibasaki J, Aida N, Morisaki N, Tomiyasu M, Nishi Y, Toyoshima K. (2018) Changes in Brain Metabolite Concentrations after Neonatal Hypoxic-ischemic Encephalopathy. *Radiology*, 288: 840–848.
75. Lucke AM, Shetty AN, Hagan JL, Walton A, Stafford TD, Chu ZD, Rhee CJ, Kaiser JR, Sanz Cortes M. (2019) Early proton magnetic resonance spectroscopy during and after therapeutic hypothermia in perinatal hypoxic-ischemic encephalopathy. *Pediatr Radiol*, 49: 941–950.
76. Peden CJ, Rutherford MA, Sargentoni J, Cox IJ, Bryant DJ, Dubowitz LM. (1993) Proton spectroscopy of the neonatal brain following hypoxic-ischaemic injury. *Dev Med Child Neurol*, 35: 502–510.
77. Groenendaal F, Veenhoven RH, van der Grond J, Jansen GH, Witkamp TD, de Vries LS. (1994) Cerebral lactate and N-acetyl-aspartate/choline ratios in asphyxiated full-term neonates demonstrated in vivo using proton magnetic resonance spectroscopy. *Pediatr Res*, 35: 148–151.
78. Hanrahan JD, Cox IJ, Azzopardi D, Cowan FM, Sargentoni J, Bell JD, Bryant DJ, Edwards AD. (1999) Relation between proton magnetic resonance spectroscopy within 18 hours of birth asphyxia and neurodevelopment at 1 year of age. *Dev Med Child Neurol*, 41: 76–82.
79. Goergen SK, Ang H, Wong F, Carse EA, Charlton M, Evans R, Whiteley G, Clark J, Shipp D, Jolley D, Paul E, Cheong JLY. (2014) Early MRI in term infants with perinatal hypoxic-ischaemic brain injury: interobserver agreement and MRI predictors of outcome at 2 years. *Clin Radiol*, 69: 72–81.
80. Boichot C, Walker PM, Durand C, Grimaldi M, Chapuis S, Brunotte F. (2006) Term neonate prognoses after perinatal asphyxia: contributions of MR imaging, MR spectroscopy, relaxation times, and apparent diffusion coefficients. *Radiology*, 239: 839–848.
81. Zhu W, Zhong W, Qi J, Yin P, Wang C, Chang L. (2008) Proton magnetic resonance spectroscopy in neonates with hypoxic-ischemic injury and its prognostic value. *Transl Res*, 152: 225–232.
82. Ancora G, Soffritti S, Lodi R, Tonon C, Grandi S, Locatelli C, Nardi L, Bisacchi N, Testa C, Tani G, Ambrosetto P, Faldella G. (2010) A combined a-EEG and MR

- spectroscopy study in term newborns with hypoxic–ischemic encephalopathy. *Brain Dev*, 32: 835–842.
83. van Doormaal PJ, Meiners LC, ter Horst HJ, van der Veere CN, Sijens PE. (2012) The prognostic value of multivoxel magnetic resonance spectroscopy determined metabolite levels in white and grey matter brain tissue for adverse outcome in term newborns following perinatal asphyxia. *Eur Radiol*, 22: 772–778.
 84. Alderliesten T, de Vries LS, Staats L, van Haastert IC, Weeke L, Benders MJNL, Koopman-Esseboom C, Groenendaal F. (2017) MRI and spectroscopy in (near) term neonates with perinatal asphyxia and therapeutic hypothermia. *Arch Dis Child Fetal Neonatal Ed*, 102: F147–152.
 85. Lally PJ, Montaldo P, Oliveira V, Soe A, Swamy R, Bassett P, Mendoza J, Atreja G, Kariholu U, Pattnayak S, Sashikumar P, Harizaj H, Mitchell M, Ganesh V, Sundeep Harigopal S, Dixon J, English P, Clarke P, Muthukumar P, Satodia P, Wayte S, Abernethy LJ, Yajamanyam K, Bainbridge A, Price D, Huertas A, Sharp DJ, Kalra V, Chawla S, Shankaran S, Thayyil S, MARBLE consortium. (2019) Magnetic resonance spectroscopy assessment of brain injury after moderate hypothermia in neonatal encephalopathy: a prospective multicentre cohort study. *Lancet Neurol*, 18: 35–45.
 86. Thayyil S, Chandrasekaran M, Taylor A, Bainbridge A, Cady EB, Chong WKK, Murad S, Omar RZ, Robertson NJ. (2010) Cerebral Magnetic Resonance Biomarkers in Neonatal Encephalopathy: A Meta-analysis. *Pediatrics*, 125: e382–395.
 87. Mitra S, Kendall GS, Bainbridge A, Sokolska M, Dinan M, Uria-Avellanal C, Price D, Mckinnon K, Gunny R, Huertas-Ceballos A, Golay X, Robertson NJ. (2019) Proton magnetic resonance spectroscopy lactate/N-acetylaspartate within 2 weeks of birth accurately predicts 2-year motor, cognitive and language outcomes in neonatal encephalopathy after therapeutic hypothermia. *Arch Dis Child Fetal Neonatal Ed*, 104: F424–432.
 88. Wilkinson D. (2010) MRI and withdrawal of life support from newborn infants with hypoxic-ischemic encephalopathy. *Pediatrics*, 126: e451-458.
 89. Bottomley PA. (1991) The trouble with spectroscopy papers. *Radiology*, 181: 344–350.
 90. Shankaran S, Pappas A, McDonald SA, Vohr BR, Hintz SR, Yolton K, Gustafson KE, Leach TM, Green C, Bara R, Petrie Huitema CM, Ehrenkranz RA, Tyson JE, Das A, Hammond J, Peralta-Carcelen M, Evans PW, Heyne RJ, Wilson-Costello DE, Vaucher YE, Bauer CR, Dusick AM, Adams-Chapman I, Goldstein RF, Guillet R, Papile LA, Higgins RD, Eunice Kennedy Shriver NICHD Neonatal Research Network. (2012) Childhood outcomes after hypothermia for neonatal encephalopathy. *N Engl J Med*, 366: 2085–2092.

91. Mwaniki MK, Atieno M, Lawn JE, Newton CR. (2012) Long-term neurodevelopmental outcomes after intrauterine and neonatal insults: a systematic review. *Lancet*, 379: 445–452.
92. Robertson C, Finer N. (1985) Term infants with hypoxic-ischemic encephalopathy: outcome at 3.5 years. *Dev Med Child Neurol*, 27: 473–484.
93. Amiel-Tison C, Ellison P. (1986) Birth asphyxia in the fullterm newborn: early assessment and outcome. *Dev Med Child Neurol*, 28: 671–682.
94. Robertson CM, Perlman M. (2006) Follow-up of the term infant after hypoxic-ischemic encephalopathy. *Paediatr Child Health*, 11: 278–282.
95. Black MM, Matula K. *Essentials of Bayley Scales of Infant Development II Assessment*, 1st edition. Wiley, Hoboken, 1999: 1–162.
96. Rosenbaum P, Paneth N, Leviton A, Goldstein M, Bax M, Damiano D, Dan B, Jacobsson B. (2007) A report: the definition and classification of cerebral palsy. *Dev Med Child Neurol Suppl*, 109: 8–14.
97. Eunson P. (2016) Aetiology and epidemiology of cerebral palsy. *Paediatr Child Health*, 26: 367–372.
98. Fejes M, Varga B, Hollódy K. (2019) [Epidemiology, cost and economic impact of cerebral palsy in Hungary]. *Ideggyogyaszati Szle*, 72: 115–122.
99. Michael-Asalu A, Taylor G, Campbell H, Lelea L-L, Kirby RS. (2019) Cerebral Palsy: Diagnosis, Epidemiology, Genetics, and Clinical Update. *Adv Pediatr*, 66: 189–208.
100. Jacobsson B, Hagberg G. (2004) Antenatal risk factors for cerebral palsy. *Best Pract Res Clin Obstet Gynaecol*, 18: 425–436.
101. Minear WL. (1956) A classification of cerebral palsy. *Pediatrics*, 18: 841–852.
102. Cans C. (2000) Surveillance of cerebral palsy in Europe: a collaboration of cerebral palsy surveys and registers. *Dev Med Child Neurol*, 42: 816–824.
103. Monbaliu E, Himmelmann K, Lin J-P, Ortibus E, Bonouvrié L, Feys H, Vermeulen RJ, Dan B. (2017) Clinical presentation and management of dyskinetic cerebral palsy. *Lancet Neurol*, 16: 741–749.
104. Graham HK, Rosenbaum P, Paneth N, Dan B, Lin J-P, Damiano DL, Becher JG, Gaebler-Spira D, Colver A, Reddihough DS, Crompton KE, Lieber RL. (2016) Cerebral palsy. *Nat Rev Dis Primer*, 2: 1–25.
105. Ikeudenta BA, Rutkofsky IH. (2020) Unmasking the Enigma of Cerebral Palsy: A Traditional Review. *Cureus*, 12: e11004.

106. Paulson A, Vargus-Adams J. (2017) Overview of Four Functional Classification Systems Commonly Used in Cerebral Palsy. *Child (Basel)* 4: 30.
107. Palisano RJ, Rosenbaum P, Bartlett D, Livingston MH. (2008) Content validity of the expanded and revised Gross Motor Function Classification System. *Dev Med Child Neurol*, 50: 744–750.
108. Nelson KB, Chang T. (2008) Is cerebral palsy preventable? *Curr Opin Neurol*, 21: 129–135.
109. Hanley JA, McNeil BJ. (1983) A method of comparing the areas under receiver operating characteristic curves derived from the same cases. *Radiology*, 148: 839–843.
110. Barkovich AJ, Hajnal BL, Vigneron D, Sola A, Partridge JC, Allen F, Ferriero DM. (1998) Prediction of neuromotor outcome in perinatal asphyxia: evaluation of MR scoring systems. *Am J Neuroradiol*, 19: 143–149.
111. Zou R, Xiong T, Zhang L, Li S, Zhao F, Tong Y, Qu Y, Mu D. (2018) Proton Magnetic Resonance Spectroscopy Biomarkers in Neonates With Hypoxic-Ischemic Encephalopathy: A Systematic Review and Meta-Analysis. *Front Neurol*, 9: 732.
112. Vannucci RC, Towfighi J, Vannucci SJ. (2004) Secondary energy failure after cerebral hypoxia-ischemia in the immature rat. *J Cereb Blood Flow Metab*, 24: 1090–1107.
113. Lei H, Peeling J. (1998) Effect of temperature on the kinetics of lactate production and clearance in a rat model of forebrain ischemia. *Biochem Cell Biol*, 76: 503–509.
114. Chan KWY, Chow AM, Chan KC, Yang J, Wu EX. (2010) Magnetic resonance spectroscopy of the brain under mild hypothermia indicates changes in neuroprotection-related metabolites. *Neurosci Lett*, 475: 150–155.
115. Nagy E, Herbert Z, Péter I, Csorba E, Skobrák A, Farkas N, Hollódy K. (2020) The usefulness of MRI Classification System (MRICS) in a cerebral palsy cohort. *Acta Paediatr*, 109: 2783–2788.
116. Moreno-De-Luca A, Ledbetter DH, Martin CL. (2012) Genetic insights into the causes and classification of cerebral palsies. *Lancet Neurol*, 11: 283–292.
117. Phelan JP, Korst LM, Martin GI. (2011) Application of criteria developed by the Task Force on Neonatal Encephalopathy and Cerebral Palsy to acutely asphyxiated neonates. *Obstet Gynecol*, 118: 824–830.
118. van Schie PEM, Becher JG, Dallmeijer AJ, Barkhof F, Van Weissenbruch MM, Vermeulen RJ. (2010) Motor testing at 1 year improves the prediction of motor and mental outcome at 2 years after perinatal hypoxic-ischaemic encephalopathy. *Dev Med Child Neurol*, 52: 54–59.

10 Bibliography of the candidate's publications

10.1 Publications related to the thesis:

Barta H, Jermendy A, Kolossvary M, Kozak LR, Lakatos A, Meder U, Szabo M, Rudas G. (2018) Prognostic value of early, conventional proton magnetic resonance spectroscopy in cooled asphyxiated infants. *BMC Pediatr*, 18: 302. doi: 10.1186/s12887-018-1269-6.

IF: 1.983

Barta H, Terebessy T, Vágó I, Dobi M, Simai A, Andorka C, Hevér D, Szabó M. (2020) [Prevalence of cerebral palsy and data quality assessment of patient documentation at the Clinics of Semmelweis University]. *Orv Hetil*, 161: 873-880. doi: 10.1556/650.2020.31722.

IF: 0.417

Barta H, Jermendy A, Kovacs L, Schiever N, Rudas G, Szabo M. (2021) Predictive performance and metabolite dynamics of proton MR spectroscopy in neonatal hypoxic-ischemic encephalopathy. *Pediatr Res*, doi: 10.1038/s41390-021-01626-z

IF: 3.756

Barta H, Terebessy T, Vágó I, Dobi M, Szegi D, Szilvay Sz, Brandt F, Andorka Cs, Hevér D, Szabó M. (2020) [Risk factors of cerebral palsy]. *Gyermekgyógyászat*, 71: 161-164.

10.2 Publications not related to the thesis:

Bajnok A, Berta L, Orbán C, Veres G, Zádori D, **Barta H**, Méder Ü, Vécsei L, Tulassay T, Szabó M, Toldi G. (2017) Distinct cytokine patterns may regulate the severity of neonatal asphyxia-an observational study. *J Neuroinflammation*, 14: 244. doi: 10.1186/s12974-017-1023-2.

IF: 5.193

Lakatos A, Kolossváry M, Szabó M, Jermendy Á, **Barta H**, Gyebnár G, Rudas G, Kozák LR. (2019) Neurodevelopmental effect of intracranial hemorrhage observed in hypoxic

ischemic brain injury in hypothermia-treated asphyxiated neonates - an MRI study. *BMC Pediatr*, 19: 430. doi: 10.1186/s12887-019-1777-z.

IF: 1.909

11 Acknowledgements

First and foremost, I would like to express my deepest gratitude to Miklós Szabó, my PhD supervisor and my mentor for the past 9 years. Besides his immense support and help not only as a supervisor, but also as a friend and a symbolic parent, he guided both my scientific work as well as the outline of my future pathways.

I am also deeply indebted to Ágnes Jermendy, a mentor and also a friend, who accompanied my path with constant helpfulness and support, and thought me the intellectual humility indispensable for a scientific career. I am grateful for Gábor Rudas, as well, for his relentless support and expert advice in all technical questions of pediatric radiology.

Moreover, I am especially grateful to Professor Attila Szabó, director of my PhD program, who encouraged me to start postgraduate studies at the 1st Department of Pediatrics.

I would like to gratefully thank the help and support of Kata Kovács and Enikő Szakmár, my colleagues and senior PhD students, who took time to guide me through the difficulties of doctoral training, even in spite of their own busy schedule, and helped me as friends.

Furthermore, I am deeply grateful to all the clinicians and nurses of the Neonatal Intensive Care Unit of the 1st Department of Pediatrics for the highly professional care of newborns, as well as to the medical staff of the Department of Neuroradiology, Medical Imaging Center, for the accurate and ready examination of infants. Despite their enormous work load, they always paid extraordinary attention to research questions and special requests. A special acknowledgement goes to Tamás Terebessy for his wholehearted guidance and expertise in questions of pediatric orthopedics.

Last but not least, I could not have completed this work without the devoted support of my family and my friends, whose help brought me through the most difficult moments of my doctoral training.